Effective anti-tumor immune response against HCC is orchestrated by immune cell partnership network that functions through hepatic homeostatic pathways, not direct cytotoxicity

Nicholas Koelsch[1,*], Faridoddin Mirshahi[2,3], Hussein F. Aqbi[4], Mulugeta Saneshaw[2,3], Michael O. Idowu[5,6], Amy L. Olex[6,7], Arun J. Sanyal[2,3,6], Masoud H. Manjili[1,6,8,*]

[1]Department of Microbiology & Immunology, Virginia Commonwealth University School of Medicine, Richmond, VA 23298, USA

[2]Department of Internal Medicine, VCU School of Medicine, Richmond, VA 23298, USA

[3]Stravitz-Sanyal Institute for Liver Disease and Metabolic Health, Richmond, VA 23298

[4]College of Science, Mustansiriyah University, Baghdad, P.O. Box 14022, Iraq

[5]Department of Pathology, VCU School of Medicine, Richmond, VA 23298, USA.

[6]VCU Massey Comprehensive Cancer Center, Richmond, VA 23298, USA

[7]C. Kenneth and Dianne Wright Center for Clinical and Translational Research, Virginia Commonwealth University School of Medicine

[8]VCU Institute of Molecular Medicine, Richmond VA 23298

[*]Corresponding Author: Masoud H. Manjili, Department of Microbiology & Immunology, VCU Massey Cancer Center, 401 College Street, Box 980035, Richmond, VA 23298, USA Phone: (804) 828-8779 email: masoud.manjili@vcuhealth.org; or Nicholas Koelsch, e-mail: koelschnj@vcu.edu;

Keywords: systems immunology, hepatocellular carcinoma, nonalcoholic fatty liver disease, cancer dormancy, inflammation, network medicine, stromal cells

Abstract

The liver harbors a diverse array of immune cells during both health and disease. The specific roles of these cells in nonalcoholic fatty liver disease (NAFLD) and hepatocellular carcinoma (HCC) remain unclear. Using a systems immunology approach, we demonstrate that reciprocal cell-cell communications function through dominant-subdominant pattern of ligand-receptor homeostatic pathways. In the healthy control, hepatocyte-dominated homeostatic pathways induce local immune responses to maintain liver homeostasis. Chronic intake of a Western diet (WD) alters hepatocytes and induces hepatic stellate cell (HSC), cancer cell and NKT cell-dominated interactions during NAFLD. During HCC, monocytes, hepatocytes, and myofibroblasts join the dominant cellular interactions network to restore liver homeostasis. Dietary correction during NAFLD results in nonlinear outcomes with various cellular rearrangements. When cancer cells and stromal cells dominate hepatic interactions network without inducing homeostatic immune responses, HCC progression occurs. Conversely, myofibroblast and fibroblast-dominated network orchestrates monocyte-dominated HCC-preventive immune responses. Tumor immune surveillance by 75% of immune cells successfully promoting liver homeostasis can create a tumor-inhibitory microenvironment, while only 5% of immune cells manifest apoptosis-inducing functions, primarily for facilitating homeostatic liver cell turnover rather than direct tumor killing. These data suggest that an effective immunotherapy should promote liver homeostasis rather than direct tumor killing.

Introduction

Classic interpretations of existing data suggest that immune responses are induced only in response to damage or infection, with the immune system being naturally tolerogenic to avoid reacting against harmless substances such as gut-derived nutrients in the liver [1]. However, emerging evidence challenges this view by demonstrating the presence of inflammatory immune responses under healthy conditions in the liver. The healthy liver maintains an active cytokine milieu, including pro-inflammatory cytokines such as IL-2, IL-7, IL-12, IL-15, TNF-α, and IFN-γ, as well as anti-inflammatory cytokines like IL-10, IL-13, and TGF-β, produced by the hepatic immune system [2]. Additionally, activated NKT cells support hepatocyte proliferation and liver regeneration [3]. Hepatic B and T cells also contribute to liver regeneration by producing lymphotoxin β (LTβ) [4,5], as the blocking of LTβR impedes liver regeneration after partial hepatectomy [6]. Human hepatic $CD141^+$ dendritic cells (DCs) are potent cytokine producers and activators of T cells [7]. This homeostatic inflammatory immune response is essential for hepatic cell regeneration and tissue remodeling. However, the mechanisms by which hepatic immune responses are induced under healthy conditions or non-alcoholic fatty liver disease (NAFLD) and hepatocellular carcinoma (HCC) remain elusive. The present study addresses this gap by the assessment of the hepatic immune system under healthy condition on a regular chow diet (CD) as well as during the progression or inhibition of HCC.

The immune system in each organ, including the liver, operates through a complex network of reciprocal cis and trans cellular interactions via ligand-receptor communications. Understanding this system requires a holistic perspective rather than focusing on individual cell types alone. This systems perspective is crucial for both the immunobiology of diseases and the development of novel immunotherapies. While reductionist approaches in immunology have advanced our

knowledge of immune cell types, they fall short in uncovering the mechanisms of emergent collective functions of the organ-specific immune system, and in offering curative immunotherapies beyond prolonging the survival of cancer patients. Recent reviews have highlighted contradictory observations regarding the dual functions of innate and adaptive immune responses in tumor immune surveillance, inflammation-associated liver protection or liver damage, and promotion or inhibition of HCC [8–10].

Recent advancements in big data and computational algorithms have enabled the detection of cellular interactions as distinct networks, providing deeper insights into disease mechanisms. By adopting a systems immunology approach for understanding the progression of NAFLD to HCC, it has been demonstrated that dominant-subdominant relationships among hepatic immune cells shape immunological patterns from which collective functions emerge, distinct from the individual roles of each immune cell type [11–13]. These dominant-subdominant interactions are analogous to "cell competition" or "cellular fitness," where winner cells survive and eliminate loser cells [14,15]. In the present study, we focused on the molecular pathways of ligand-receptor interactions to uncover immunological patterns associated with dominant cell types and pathways involved in the progression or inhibition of HCC in the DIAMOND mouse model. This approach allows for a more comprehensive understanding of the mechanisms of NAFLD and HCC, as well as the development of more effective therapeutic strategies. Such interactions network analysis of hepatic cells revealed the presence of carcinogenic processes prior to the formation of HCC on a WD as well as during rescue from HCC through dietary correction, indicating the presence of dormant cancer. Additionally, cellular partnership that promoted liver homeostatic pathways was found to be a crucial mechanism of hepatic immune surveillance for preventing HCC.

Results

Carcinogenic events take place during NAFLD and remain dormant during rescue from HCC

The livers of male DIAMOND mice that were on a CD or a WD or reversal of a WD to a CD for 12 weeks starting from 36 weeks of being on a WD were examined and subjected to hematoxylin-eosin (H&E) staining and single nuclei RNA sequencing (snRNAseq) analysis when animals reached 13 months of age. There was no macroscopic or microscopic tumor detectable in the liver of animals during NAFLD at 11 months of age (WD.nf) or rescue from HCC following diet correction at 13 months of age (RD.n) (Figure 1A). However, cell annotation and UMAP clustering of non-immune cells revealed a cancer fraction in the liver (Figure 1B), characterized by the signature of alpha-fetoprotein (AFP), hepatocyte nuclear factor 4 alpha (HNF4α) and glypican-3 (GPC3), separating them from hepatocytes (Figure S1, Figure 1C). Further filtration of the cancer fractions based on the expression of GPC3 transcript, which is more sensitive than AFP in the diagnosis of liver cancer [16], revealed the expression of all three markers in the WD.nf and WD.t groups while the RD.t and RD.n expressed two markers (Figure 1D). Among these groups, high level of HNF4α transcript in the RD.n group (Figure 1E) was associated with recovery from HCC (Figure 1A) whereas low level of HNF4α transcript in the WD.nf and RD.t groups (Figure 1E) was associated with NAFLD and HCC, respectively (Figure 1A). In the CD group, the tumor suppressor HNF4α [17] was at the highest levels compare to other groups (Figure 1E). Progression of HCC in the RD.t group could be due to epigenetic memory that might be established during a WD since a transient inflammatory event could establish epigenetic memory and induce cellular transformation [18,19]. It is yet to be determined whether

such malignant events signify tumor dormancy or the presence of cancer stem cells. We have previously detected such tumor dormancy in the FVBN202 transgenic mouse model of breast cancer [20].

Hepatic structural cells directly induce immune responses to maintain liver tissue integrity through homeostatic pathways

We aimed to investigate the crosstalk between hepatic structural cells and immune cells during liver tissue homeostasis under normal physiological conditions. To achieve this, we analyzed the livers of one-year-old mice that had been on a regular CD for 40 weeks, using scSorter and CellChat Analyses. Although immune cells were quantitatively dominated by B cells, T cells and macrophages (Figure 2A), the receptor-ligand interaction analyses revealed that 75% of macrophages and monocytes were active in cell-cell interactions whereas only 25% of B and T cells participated in the cellular interactions network (Figure 2B-C). In fact, 75% and 25% of each cell type contributed 8 and 35 dominant signals through the ligand-receptor interaction network, respectively (Figure 2B-C). These data suggest that cellular dominance is determined by the ligand-receptor interactions rather than the frequency of cell types being present in the immune pattern. Then, we focused on the signaling communications between hepatic nonimmune cells and immune cells. To this end, 75% of macrophages communicated with cholangiocytes, HSCs and myofibroblasts as well as 75% of monocytes communicating only with hepatocytes (Figure 2D), while other immune cells accounted for the 25% of cellular interactions network (Figure 2E). In the liver-induced immune cell activation front, hepatocyte-dominated liver structural cells activated immune cells through the hepatic homeostatic pathways including GAS, galectin 9, spp1, collagen, laminin and DHEAS (Figure 2D-E). The 75% majority of macrophages received GAS signaling from 75% of cholangiocytes and 25% of

myofibroblasts (Figure 2D-E, Table S1A-B). GAS signaling can promote efferocytosis of macrophages [21,22]. Also, 25% of the hepatic immune cells can be activated through CD45, CD44 and VLA-4 by different hepatic structural cells producing galectin, spp1, collagen and laminin (Figure 2E). Galectin-9 has been reported to induce T cell activation through the engagement with the dominant pathway CD45 that regulates signaling thresholds by dephosphorylating components of the Src kinase family, and LcK-dependent calcium mobilization in peripheral $CD4^+$ T cells [23]. Also, the Galectin 9-CD44 interaction enhances stability and function of adaptive Tregs [24]. Finally, Galectin 9 binds IgM-BCR to regulate B cell signaling [25]. Targeting Dag1 can activate phospholipase C gamma (PLC-γ) downstream of the TcR-CD1d in NKT cells [26]. Hepatocytes also modulated immune responses through the anti-inflammatory DHEAS that targeted Pparα [27,28] (Figure 2E). Activation of DCs, T cells, B cells and NK cells by hepatic structural cells was also detected in 5% of cells through the pathways involving Flt-3, IL-2 pathway (IL7/IL15) and IL-16 (Figure S2A). Along this line, flow cytometry analysis of the hepatic T cells showed presence of $CD44^+/CD62L^{-/low}$ $CD4^+$ Te and $CD8^+$ Te cells in the liver (Figure 2F). Consistent with our observations, it was reported that both $CD4^+$ and $CD8^+$ T cells, but not γδ T cells, are required for normal liver regeneration through lymphotoxin production such that $RAG1^{-/-}$ mice show extensive hepatic injury following partial hepatectomy [4].

In the liver homeostatic front, immune cells participated in liver tissue homeostasis through the homeostatic pathways which included IGF, FN1, VTN, PROS, DHEA, IL-1β and cholesterol (Figure 2D-E). The 75% majority of macrophages sent IGF signaling to 75% of HSCs and myofibroblasts, and to 25% of DCs and all other hepatic structural cells (Figure 2D-E, Table S1C-D). Among 25% of cells, monocytes, neutrophils and DCs joined macrophages in sending IGF signaling to hepatic structural cells, as well as 25% of DCs receiving this signal from

macrophages, hepatocytes and stromal cells (Table S1D). The IGF-IGFR1 pathway is involved in normal glucose homeostasis in the liver [29], the activation of myofibroblasts and HSCs, as well as modulation of DC maturation [30]. Also, 75% of monocytes sent FN1 signaling to 75% of hepatocytes for their regeneration through SDC4 [31] while receiving no signal from other cells (Figure 2D, Table S1E). In 25% cells, FN1 pathway was reciprocally used by immune cells and nonimmune cells to induce activation of immune cells as well as homeostatic of nonimmune cells (Table S1F). Cholesterol targeting RoRα induces fatty acid oxidation and modulation of inflammation in immune cells [32,33] during activation of T cells, DCs, NK cells, NKT cells, monocytes and neutrophils [34,35] as well as liver structural cells for hepatic lipid homeostasis [36]. Finally, hepatic immune cells participated in homeostasis of liver cells through production of VTN and PROS (Figure 2E). The VTN signaling can prime macrophage-related inflammation [37], and inhibit phagocytic efferocytosis of macrophages [38]. Finally, 25% of macrophages and neutrophils dominated IL-1β signaling to HSCs and hepatocytes (Figure 2E). IL-1β can stimulate cholesterol accumulation in hepatocytes [39] (Figure 2E) as well as proliferation and survival of HSCs [40]. These data suggest that over 75% of macrophages and monocytes as well as 25% of other immune cells participated in liver homeostasis. Also, 5% of immune cells participated in turnover of the hepatic structural cells through TRAIL and Fas-L pathways (Figure S2A).

Among 75% of structural cells, hepatocytes, HSCs, cholangiocytes, myofibroblasts, fibroblasts, endothelial cells, and LSEC were dominant in liver tissue homeostasis by producing GAS, IGF, FN1, PARs, laminin, collagen, sema-3, and ANGPT (Figure 2B, D, Figure S2B). These data suggest the tissue-based direct activation of the immune cells as well as engagement of activated immune cells in liver homeostasis during normal condition.

HCC progression or inhibition is driven by hepatic cellular interaction networks modulating liver microenvironment through NKT cell and monocyte-dominated immune responses, not direct tumor targeting

In order to determine immune cell infiltrates into the liver during health and disease as well as during recovery from HCC, proportions of immune cells and nonimmune cells were analyzed. While immune cells were at the lowest ratio to nonimmune cells in the CD group, the ratio increased during a WD and dietary correction such that the highest ratio of immune cells to nonimmune cells was detected during dietary correction (Figure 3A). Then, we hypothesized that immune cell infiltrations were of host-protective nature during hepatic damages induced by a WD such that immune infiltrates even increased further during diet reversal to continue restoring the liver integrity. To test this hypothesis, ligand-receptor interactions representing 75% of hepatic cells were analyzed as representation of the hepatic immune functions. The highest number and strength of ligand-receptor interactions were evident during NAFLD or HCC on a WD as well as rescue from HCC following diet reversal (Figure 3B). In order to identify cell types that dominate the communication networks under each condition, cell type ratios and cell-cell interactions were analyzed. In all groups, hepatocytes and macrophages were dominant cell populations compared to other nonimmune and immune cell types (Figure 3C, left panels). However, the CD group showed no cell-cell communications above a cut-off signal strength of 2, below which hepatocytes and myofibroblasts dominated cell-cell communications network (Figure 3C, right panel). In all other groups, cellular dominance in the ligand-receptor interactions differed from the cell frequency dominance. Among immune cells sending signals to other cells, NKT cells were dominant during NAFLD while NKT cells and monocytes were dominant during HCC on a WD (Figure 3C, right panels). No immune cell dominance was

detected during HCC on a RD, while monocytes dominated immune cell interactions network during rescue from HCC (Figure 3C, right panels). Among nonimmune cell communications network, cancer cells were dominant during NAFLD while myofibroblasts, cancer, hepatocytes, and fibroblasts became dominant during HCC on a WD. Following dietary correction, cancer cells remained dominant during HCC whereas myofibroblasts, fibroblasts, hepatocytes and cancer cells became dominant during rescue from HCC (Figure 3C, right panels). These data suggest that cancer cells, both as dormant and proliferating tumor, remain dominant in the ligand-receptor interactions network. Similar trends were detected in 25% of the hepatic cells (Figure S3A). However, among nonimmune cells, HSCs were dominant in the CD group as well as stromal cells becoming dominant during HCC on a WD or RD (Figure S3B). Overall, these data suggest that dominant ligand-receptor cellular partnership networks are more important than the number of immune cell infiltrates such that the highest proportion of immune cell infiltrates with the lowest number of cellular interactions partnership failed to rescue animals from HCC following a dietary correction in the RD.t group, unless the number of ligand-receptor interactions increased in the RD.n group (Figure 3A-B). The highest number and strength of cellular interactions in the WD.t group (Figure 3B), which failed to prevent HCC, was perhaps because of continuous intake of a WD which can overwhelm the host-protective immune responses. Although there are contradictory reports on the role of NKT cells as well as T cells, macrophages, and monocytes in promoting or inhibiting HCC [41–48], our data suggest that NKT cells became dominant to protect against NAFLD, but they failed to succeed because of chronic intake of a WD, as NKT cells disappeared following diet correction. Also, monocytes, neutrophils, T cells, NK cells and DCs were active in sending signals for protecting from HCC in the WD.t group, but they did not succeed because of chronic intake of a WD; however, retention

of the immune cell activities during diet correction rescued animals from HCC, whereas inability to mount immune responses in sending signals resulted in HCC progression following dietary correction.

HSCs, cancer cells and NKT cells dominate cellular interactions network with NKT cells orchestrating the hepatic immune responses mainly through homeostatic pathways during the progression of NAFLD on a WD

We have previously reported that collective function of the hepatic structural cells or immune cells is determined by dominant-subdominant interactions within the cellular networks [11–13]. Here, we sought to determine molecular pathways that dominate cell-cell interactions during the progression of NAFLD. To do this end, comparative analyses of the ligand-receptor interactions in the CD and WD.nf (NAFLD) groups representing 75% of each cell population as well as subdominant 25% of cell population were performed. For the majority of nonimmune cells, HSCs and cancer cells dominated the ligand-receptor cellular partnership network by increasing the outgoing and incoming signals during the progression of NAFLD compared with those during a CD (Figure 4A-B). Among immune cells, NKT cells became dominant in sending and receiving signals followed by monocytes and macrophages only receiving signals during NAFLD (Figure 4A-B). Such cell-cell communication partnership dominated by these cells was evident despite the highest proportion of hepatocytes and macrophages during NAFLD (Figure 4A). A comparative analysis of signaling interactions for these three dominant cells (Figure 4C) showed emerging additional hepatic homeostatic pathways during NAFLD which were absent in the CD group (Figure 4D). These cells also upregulated MHC class I compared to those in the CD group, as well as monocytes and macrophages upregulating MHC class II during NAFLD (Figure S4). HSCs induced activation of NKT cells as well as macrophages and monocytes

through liver homeostatic pathways involving collagen, laminin, FN1 interacting with the co-stimulatory VLA-4, as well as the LcK activating CD45 and CD44 [49,50], SDC4 and Dag-1 (Figure 4E, Table S2A-B). HSCs also modulated myofibroblasts through BMP and HGF [51] (Figure 4E). NKT cells and cancer cells activated all immune cells through galectin 9 engaged with CD44, CD45, Ighm and P4HB (Figure 4F, Table S3A, Table S4A) for participating in homeostasis of the hepatic nonimmune cells through PARs, testosterone, cholesterol and 27HC signaling, as well as the induction of angiogenesis through VEGF (Figure 4F, Table S3B and Table S4B). Such T cell and NKT cell activation were associated with increased expression of hepatic MHC class I and II as well as CD1d during NAFLD (Figure S4). Seventy five percent of all immune cells other than NKT cells did not send any additional signal to other cells (Figure S5A). All hepatic cells except for fibroblasts and hepatocytes, as well as all immune cells were impacted by NKT cells and cancer cells sending signals to them (Figure 4C, Figure S5A-B).

Analysis of 25% of cell types showed similar pattern of dominance for HSCs, cancer cells and NKT cells in the ligand-receptor interactions network during NAFLD (Figure S6A-B). Other hepatic nonimmune cells and immune cells exhibited a similar pattern of activity to that of 75% of NKT cells and HSCs, dominating their communications with NKT cells and cancer cells. The exception was hepatocytes and fibroblasts, whose communication remained disrupted (Figure S6B). These data suggest that the communication network was disrupted mainly in 75% hepatocytes and fibroblasts (Figure S5B) being detectable even in 25% of hepatocytes and fibroblasts (Figure S6B). Only 25% of other immune cells, including macrophages and monocytes, remained active (Figure S6A), which also upregulated MHC class I and II (Figure S4). Consequently, NKT cells had to compensate for other immune cells in supporting hepatic homeostasis, leading to them being overwhelmed by the constant intake of a WD. Even 5% of

NKT cells did not show direct Fas or TRAIL-mediated apoptosis-inducing function against cancer cells while NK cells and T cells utilized these mechanisms mainly for hepatic structural cells turnover (Figure S7). Hepatic structural cells were still engaged in the activation and differentiation of immune cells through Flt-3 and IL-7/IL-15 pathways (Figure S7).

The hepatic cellular interaction networks dominated by cancer cells, hepatocytes, myofibroblasts and fibroblasts induce NKT cell and monocyte-dominated immune responses mainly through liver homeostatic pathways during HCC on a WD

Analysis of the pattern of the ligand-receptor interactions in 75% of liver cells showed cancer, hepatocytes, myofibroblasts and fibroblasts dominating the signaling network along with immune cells dominated by NKT cells and monocytes during the progression of HCC on a WD (Figure 5A). Such cell-cell communication dominance was detected despite the highest proportion of hepatocytes and macrophages during NAFLD (Figure 5A). In order to determine signaling pathways induced in the presence of HCC, comparative analyses between the WD.t vs. WD.nf groups were performed. Among these four dominant nonimmune cells, hepatocytes and fibroblasts, which did not interact with NKT cells during NAFLD (Figure 4 and Figure S5), dominantly communicated with NKT cells (Figure 5B-C), whereas cancer and myofibroblasts shifted from communicating with NKT cells during NAFLD (Figure 4 and Figure S5) to communicating with monocytes during HCC (Figure 5B-C). All these dominant cells upregulated CD1d during HCC (Figure S8A), which could present glycolipid to NKT cells for their activation. Among other hepatic cells, stromal cells that did not show active communications during NAFLD (Figure S5B), dominated their communications with NKT cells during HCC on a WD (Figure S8B). Other hepatic cells sent dominant signals to NKT cells while received signals mainly from monocytes (Figure S8B). While monocytes and all other

immune cells were impacted by myofibroblasts, NKT cells were mainly impacted by stromal cells (Figure 5C and Figure S8B). Monocytes with reduced signaling to other cells during NAFLD (Figure S5A), showed additional signaling to all hepatic cells during HCC (Figure 5C). Among these dominant cells, 75% of fibroblasts did not interact with hepatic cells during NAFLD whereas they communicated homeostatic and immune activating signals during HCC on a WD (TableS5A-B). Hepatocytes that only sent PARs signal to cancer, myofibroblasts, HSCs, cholangiocytes and NKT cells during NAFLD, they sent several tissue homeostatic signals to all hepatic nonimmune cells as well as several immune modulatory signals to NKT cells, monocytes and macrophages (Table S5C-D). Myofibroblasts expanded their homeostatic signaling to hepatocytes and fibroblasts as well as activating signals to all other immune cells during HCC (Table S5E-F). Finally, 75% of stromal cells that did not show any signaling communications during NAFLD, began affecting hepatic cells as well as macrophages and NKT cells but not monocytes (Table S5G-H). These data suggest that stromal cells are associated with tumor progression whereas myofibroblasts and monocytes function to inhibit HCC. Similar patterns of cellular dominance were detected in 25% of each cell type, though stromal cells also become dominant in cell-cell signaling network (Figure S9A-C).

Analysis of signaling pathways showed that cancer cells and NKT cells maintained PARs and FN1 signaling during HCC, though PARs targeted additional cell types including hepatocytes, fibroblasts and monocytes, and FN1 also targeted additional cells including fibroblasts, myofibroblasts and hepatocytes during HCC (Figure 5D, Table S6). Cancer cells showed new signals with PARs signaling being dominant over FGF, DHEAS, NRG, CypA, AGT, PROS, as well as NKT cells showing dominant PARs signaling over CypA, VTN, AGT, NRG and Spp1 (Figure 5D). Hepatocytes, myofibroblasts, fibroblasts and monocytes, all showed, mainly

additional new signals during HCC, among which PARs was the strongest new signaling communication received by hepatocytes, sent by myofibroblasts, or sent/received by fibroblasts and monocytes (Figure 5D). These signaling pathways are involved in cell growth and survival, cell regeneration and repair, and immune cells activation. PARs signaling facilitates cell polarity and tight junctions which are essential for maintaining the integrity of the liver tissue. During liver injury on a WD, PARs signaling facilitates hepatocytes repair and regeneration process. On immune cells, PARs signaling promotes phagocytosis of macrophages and monocytes through the formation of the phagocytic cup, as well as the formation of the immune synapse, facilitating effective cell-cell communication and T cell activation. These dominant cells also induced angiogenesis in endothelial cells and LSEC by producing VEGF (Figure 5D). These data suggest that tumor progression was because of continuous intake of a WD that overwhelmed anti-tumor immune responses, rather than immune escape mechanisms since MHC class I and CD1d were upregulated during HCC progression compared to those during NAFLD, with only T cells, monocytes and macrophages downregulating MHC class II while B cells retaining it (Figure S8A & D).

Stromal cell and cancer cell-dominated interactions network promotes HCC whereas myofibroblast, fibroblast and monocyte-dominated interaction network involving homeostatic pathways orchestrate HCC preventive immune responses following dietary correction

In order to determine whether correction of diet during NAFLD can rescue animals from HCC and restore immunological pattern similar to that in the CD control group, animals were switched to a CD after 36 weeks of being on a WD. Analysis of the pattern of the ligand-receptor interactions in 75% of liver cells showed that the outcome of dietary correction depended on

rearrangements of hepatic cellular interactions network such that a dominant stromal cell and cancer cell communications, along with failure to maintain hepatic immune responses resulted in tumor progression, whereas a dominant myofibroblast and fibroblasts along with monocyte-dominated immune responses rescued animals from HCC (Figure 6A-B). NKT cells that were dominant during WD, lost their dominance following a dietary correction, suggesting that their dominance was due to a WD. Again, such dominant cell-cell communication networks were detected despite the highest frequency of hepatocytes and macrophages in these groups (Figure 6A).

Analysis of the ligand-receptor interaction networks showed that dominant stromal cells communicating with cancer and monocytes during HCC, shifted their communications with myofibroblasts and fibroblasts during rescue from HCC (Figure 6C). Similarly, dominant cancer cells communicating with stromal cells during HCC, shifted toward communications with myofibroblasts and fibroblasts during rescue from HCC (Figure 6C). Dominant myofibroblasts, fibroblasts, and hepatocytes during rescue from HCC mainly communicated with one another, as well as with monocytes whereas they were not as active in communicating additional signals during HCC progression (Figure 6C). HSCs, cholangiocytes, endothelial cells and LSEC also followed similar pattern by mainly communicating with myofibroblasts, fibroblasts and monocytes during rescue from HCC, but not much active during HCC progression (Figure 6D). For immune cells, monocytes being dominant receiver of signals (Figure 6A), were impacted mainly by stromal cells and cancer cells during HCC whereas they mainly communicated with myofibroblasts and fibroblasts during rescue from HCC, as did macrophages, T cells and B cells by sending and receiving signals, as well as DCs sending signals (Figure 6E). All immune cells received signals from stromal cells only during HCC but not during rescue from HCC (Figure

6E). NKT cells, NK cells and neutrophils showed no detectable additional signaling pathways during HCC while they sent additional signals mainly to myofibroblasts and monocytes during rescue from HCC (Figure 6E). Also, myofibroblasts and fibroblasts upregulated MHC class I and CD1d as well as B cells upregulating MHC class II during rescue from HCC compared to those during HCC progression following RD (Figure S10). Altogether, these data suggest stromal cell and cancer cell-dominant signaling network can drive HCC progression while myofibroblast, fibroblast, and monocyte-dominated network protects animals from HCC following dietary correction.

In order to detect molecular pathways of the ligand-receptor interactions for dominant cells as well as all other subdominant cells, comparative analyses of the CD group versus the RD group as well as the RD.t group versus RD.n group were performed. Stromal cells showed the highest numbers of additional new signals during HCC progression which included PARs, galectin, DHEAS, 27HC, FN1, IGF, ANGPTL and PROS (Figure 7A). These signals switched to cholesterol, FGF, VTN and retaining FN1 signal (Figure 7A) such that cholesterol and FGF were the main new additional signals received by stromal cells during rescue from HCC (Figure 7A). Cancer cells followed similar pattern with cholesterol and FGF being sent and received by stromal cells during rescue from HCC (Figure 7A). Contrary to stromal cells or cancer cells, myofibroblasts, fibroblasts and hepatocytes showed increased additional new signals only during rescue from HCC (Figure 7A). In the immune cells front, NKT cells and NK cells did not show any additional signals during HCC but they sent three new additional signals (PARs, FN1, VTN) during rescue from HCC (Figure 7B). Monocytes mainly received additional new signals during HCC whereas they impacted other cells by sending out new additional signals during rescue from HCC (Figure 7B). Macrophages followed similar trends as monocytes (Figure 7B). Among

these signals, IGF signaling targeted myofibroblasts only during HCC whereas testosterone, FGF, HGF, cholesterol, NRG, CypA and Spp1 targeted mainly dominant cells (monocytes, myofibroblasts, fibroblasts, hepatocytes, cancer cells) only during rescue from HCC (Figure 7C, Table S7A-H). To this end, IGF signaling is a major oncogenic event in many cancers, including HCC [52]. On the other hand, testosterone could induce apoptosis in tumor cells, FGF and HGF can support liver cell regeneration, as well as CypA and Spp1 activating monocytes and myofibroblasts, all of which were detected only during rescue from HCC (Figure 7C, Table S7A-H). These data suggests that restoration of the innate immune responses dominated by monocytes protect animals from HCC during dietary correction. Analysis of 25% of the hepatic cell signaling showed similar trend of cellular dominance during diet reversal (Figure S11). Since we detected new cellular rearrangements in the RD.n group which differed from those in the CD group, we asked whether molecular pathways also presented new rearrangements. Analysis of the cell-cell interaction pathways revealed that rescue from HCC following dietary correction did not restore the molecular pathways present in the CD group, rather new molecular rearrangements emerged. For instance in 75% of hepatic cells, the ligand-receptor cellular interactions in the CD group included IGF, GAS, laminin, collagen, sema-3 and ANGPT (Figure 8A) which were not detected in the RD.n group rescued from HCC and NAFLD; instead, the RD.n group showed the signaling pathways that were absent in 75% of the CD group including galectin, DHEAS, testosterone, 27HC, HGF, FGF, PROS, ANGPTL, VTN, cholesterol, NRG, CypA, Spp1, BMG and VEGF (Figure 8B). Even in 25% of the hepatic cells, sema-3 was detected only in the CD group but complement and CypA were detected only in the RD.n group (Figure 8C-D).

Discussion:

Under the influence of toxins including a chronic consumption of high fat and high sugar WD, the liver is subjected to a range of metabolic stresses and inflammatory signals that can initiate early carcinogenic processes [53], which remain dormant before the formation of HCC. We have previously reported the presence of cancer cell dormancy in the FVBN202 transgenic mouse model of spontaneous breast cancer [20] as well as the DIAMOND model of NAFLD progression to HCC [11]. Here, we took multicellular networks immunology approach to study how immune cells interact within complex cellular networks to coordinate hepatic immune responses. We demonstrated the presence of dormant cancer cells during NAFLD and prior to the formation of HCC on a WD, as well as during rescue from HCC following dietary correction. These cancer cells were actively involved in cell-cell communications network with the hepatic nonimmune cells and immune cells.

Taking a systems immunology approach, we have previously demonstrated that the immunological patterns reflecting collective immune functions during health and disease, can be understood through detection of dominant-subdominant interactions network among hepatic immune cells as well as nonimmune cells [11–13]. Such dominant-subdominant interactions have been reported in different settings as “cell competition” or “cellular fitness” in which the winner cells survive and eliminate the loser cells [14,15]. Here, we demonstrated that dominant cells do not necessarily eliminate subdominant cells, rather they orchestrate their fate of action by shifting their cellular partnership to be aligned with those of the dominant cells. Cellular dominance is more about ligand-receptor interactions network or cellular partnership rather than the number of cells since stromal cells and myofibroblasts being at low numbers dominated the cellular interactions network during HCC progression or rescue from HCC. By taking this approach, we discovered immune responses in the liver directly induced by the hepatic nonimmune cells

producing cell-matrix proteins and integrins to engage with CD44, CD45, VLA-4 and Dag-1 on immune cells for their participation in liver tissue homeostasis. To this end, monocytes and macrophages were dominant immune cells as well as 25% of all other immune cells including T cells, B cells, DCs, neutrophils, NK cells and NKT cells appeared to follow monocytes and macrophages leads in participating in liver tissue homeostasis. Only 5% of T cells, NKT cells and NK cells produced TRAIL or Fas-L, not for targeting the tumor but for targeting the hepatic structural cells turn over as hepatic homeostasis. Such tissue-based activation of the immune response is evident from the presence of tissue-resident T memory cells (Trm) [54] which can be explained by the quantum model of T cell activation recently proposed by the last author [55]. Also, the primary function of immune responses has been proposed to be participating in homeostasis of their target cells [56–61]. This homeostatic function can explain the observations on inability of auto-reactive T cells to induce autoimmune pancreatitis following adoptive transfer of OVA-specific T cells that recognized and became activated by OVA-expressing pancreas [62]. Such homeostatic immune responses were elevated during NAFLD or HCC in order to support liver cell integrity which was disrupted by a WD. The success of dietary correction in rescuing animals from HCC depended on the retention of immune responses participating in liver homeostatic pathways rather than being cytotoxic against the tumor. Our findings are consistent with recent report on Resmetirom for the treatment of patients with metabolic dysfunction-associated steatohepatitis (MASH) through restoring liver homeostasis [63].

During NAFLD, 75% of HSCs and cancer cells, as well as NKT cells dominated cell-cell interactions network whereas stromal cells, fibroblasts, hepatocytes, macrophages, monocytes and NK cells showed reduced signaling communications compared with those in the CD control group. In 25% of cells, all immune cells and nonimmune cells followed similar ligand-receptor

interactions as for dominant cells. These data suggest that NKT cells are activated by a WD during which the expression of CD1d increased to support liver homeostasis, but failed to succeed because of being overwhelmed by chronic intake of a WD. The dominance of NKT cells in orchestrating cell-cell signaling network, disappeared following reversing to a CD, indicating the induction of NKT cells by a WD. CD1d-restricted Vα14Jα18 mouse hepatic NKT cells constitute up to 10% of the leukocyte fraction in the liver or up to 40% of the hepatic lymphocytes [64]. The role of hepatic $CXCR6^+$ NKT cells in inhibiting NAFLD progression to HCC was reported in male C57BL/6J mice [65]. Such hepato-protective role of NKT cells was more pronounced in males compared to female mice model of NAFLD [41]. The host-protective role of NKT cells has also been reported in fast food diet (FFD)- and methionine choline-deficient (MCD) diet-induced mouse models, but chronic administration of α-GalCer induced NKT cell anergy and disease progression [42], suggesting that NKT cells can be overwhelmed by chronic intake of a WD. In patients with hepatic steatosis, NKT cells are significantly increased in the liver and blood [66]. During HCC progression on a WD, all nonimmune cells and immune cells became engaged, with stromal cells communication signals becoming dominantly associated with tumor progression such that their dominant signaling continued during the progression of HCC even after dietary correction, whereas they were replaced with myofibroblasts signaling dominance during rescue from HCC. Myofibroblasts are known to be major contributors to remodeling of the ECM for liver repair, which could lead to fibrinogenesis when become chronic, but they have also been shown to hinder tumor growth by mechanical restriction of tumor spread through type I collagen production [67], as well as the expression of cytoprotective molecule cytoglobin (Cygb) to reduce oxidative stress [68]. They can also detoxify

the liver by producing antioxidants and detoxifying enzymes, thereby reducing ROS levels and other toxic metabolites for supporting liver function.

In the immune cells front, inability to maintain active immune responses during diet reversal resulted in HCC progression, whereas domination of monocytes orchestrated other immune cells for participating in liver tissue homeostasis and rescue from HCC. These data suggest that disease progression or rescue from HCC does not follow a linear cause-effect direction, rather they are orchestrated through reciprocal cis and trans ligand-receptor interaction networks dynamically changing the immune system such that diet correction may fail or succeed in rescuing the host from HCC in isogenic mice, let alone in allogeneic humans. Also, when rescued from HCC, the immune pattern did not return to the CD control condition, rather a new arrangement emerged. Therefore, healthy control may not be a proper control for the efficacy of treatments, and grouping the treatment arms based on similarity and differences in the immune pattern associated with the outcome would be more biologically relevant than stratifying them into healthy control and treatment groups. Progression of HCC in the RD.t group could be due to epigenetic memory that might be established during a WD since a transient inflammatory event could establish epigenetic memory and induce cellular transformation [18,19]. Therefore, manipulating one immune cell component, especially T cells which were not found to be dominant, could be controlled by the dominant cell-cell interactions in the tumor microenvironment resulting in the failure of immunotherapeutic to cure disease.

Even in isogenic DIAMOND mice of the same sex, a single dietary change can lead to different outcomes, let alone in allogeneic humans. These findings suggest that personalized medicine is the best option for understanding the mechanisms of HCC progression or inhibition and for developing personalized immunotherapies. Consequently, randomizing patients into treatment

and healthy groups may not be the best strategy to assess the efficacy of immunotherapies, as each patient could respond differently. It remains to be determined whether the initial state of hepatic cell-cell communications might determine the outcome of each treatment.

Materials and Methods:

Mice and Sample Collection: Diet-induced animal model of nonalcoholic fatty liver disease (DIAMOND) [69] were used in this study, which are an isogenic cross between C57BL/6J and 129S1/SvImJ mice. In brief, male mice (n=2-5/group) were put on a standard CD for 40 weeks, WD, or underwent diet reversal (RD) after being on a WD. A WD consists of high fructose and glucose sugar water in conjunction with high-fat diet. Mice were on a WD for 40 weeks prior to the development of HCC and during NAFLD (the WD.nf group) or after development of HCC by 48-60 weeks (WD.t). Separate groups underwent diet reversal for additional 12-24 weeks, after 36 weeks of being on a WD, in which some mice developed tumors (RD.t) and some were rescued from the development of HCC and exhibited normal livers (RD.n).

Hematoxylin and eosin staining. Formalin fixed paraffin embedded liver (FFPE) tissues were subjected to hematoxylin and eosin (H & E) stain using Tissue Tek Prisma Autostainer as previously described by our group [70]. Histology slides were scanned at 40x magnification.

Flow Cytometry: Multicolor staining and flow cytometry analysis of T cells were performed as previously described by our group [13]. Briefly, Fc blocker anti-CD16/32 Ab was used for all staining panels before using the T cell staining panel (CD8, CD4, CD44, CD62L). All reagents were purchased from Biolegend (San Diego, CA). All reagents were used at the manufacturer's recommended concentration. Multicolor data acquisition was performed using a LSRFortessa X-20 (BD Biosciences) and a ImageStreamX Mark II Imaging Flow Cytometer (Millipore Sigma, Billaerica, MA). Data were analyzed using FCS Express v5.0 (De Novo Software; Glendale,

CA). The FVS negative viable cells were gated on CD4+ or CD8+ T cells, and analyzed for $CD44^{+}CD62L^{-//low}$ T effector (Te), $CD44^{+}CD62L^{+/high}$ (Tcm) and $CD44^{-}CD62L^{+}$ T naïve (Tn) subsets.

Quality Control and Filtering: Single nuclei RNA-seq data from all samples was provided by the Novogene company, in which nuclei were isolated from frozen mouse liver and tumor samples, and using 3' single cell gene expression libraries. Novogene performed unique molecular identifier (UMI) collapsing, alignment to mouse reference genome mm10-5.0.0, and UMI counting and initial quality control. Additionally, Novogene used Cell Ranger version 7.0.0 and introns were included in the analysis. Seurat version 4.4.0 [71] was used to handle all data and perform quality control and filtering metrics. In brief, samples were loaded into the VCU HPRC core clusters to mark data with group identifying labels (CD, WD.nf, WD.t, RD.t, RD.n), and filter cells with nFeature_RNA > 200 and < 5000, as well as for cells expressing < 5% mitochondrial associated genes. The threshold for nFeatureRNA > 200 and < 5000 is to ensure there are sufficient molecular transcripts in one cell and 5000 > may entail two cells in one run, whereas mitochondrial gene percentages higher than 5% may be indicative of dead/dying cells. High Performance Computing resources provided by the High Performance Research Computing (HPRC) core facility at Virginia Commonwealth University (https://hprc.vcu.edu) were used for conducting the research reported in this work.

Cell Type Annotation and Quantification: Markers for major liver cell types specific for mice from liver focused data were extracted from the CellMarker 2.0 database [72] and compiled into one comprehensive list to annotate cells. The scSorter R program version 0.0.2 [73] was used in conjunction with these marker genes to annotate liver immune and non-immune cell types such as B cell, T cell, DC, NKT, NK, neutrophil, monocyte, macrophage, endothelial, LSEC, stromal,

HSC, fibroblast, myofibroblast, cholangiocyte, hepatocyte, and cancer cells. Following annotation, the cells were clustered and visualized in Seurat with UMAP. Cellular annotations were confirmed by making heatmaps of marker genes specific for each cell type of interest. Further, quantification of the exact number of cells was performed in excel and normalized to 100% to show the composition of cell types in each group in the study, such as immune cells and non-immune cells. Heatmaps of specific marker genes in various cell type populations across groups were visualized and quantified in Seurat with the DoHeatmap function.

Differential Expression and IPA Analyses: DESeq2 version 1.40.2 [74] was utilized to perform differential expression analyses on individual cell type populations, as well as the collective immune or non-immune cell compartments to extract log fold change and statistical measures for each comparison of interest. Results from DESeq2 were then uploaded to Ingenuity Pathway Analysis (IPA) to evaluate molecules of interest after filtering on p-values <0.01 and z-scores of 2. The comparisons for WD.t vs. RD.t B and T cell populations yielded no molecules for IPA analysis at a p-value threshold <0.01 and were excluded from analysis due to no significant molecules being detected. IPA analysis results were focused on the major pathways detected, disease related functions, and cytokines.

Intercellular Communication Networks: CellChat version 2.1.1 (https://doi.org/10.1101/2023.11.05.565674) was utilized with default parameters (trimean approach requiring 25% of the cells in a population to express a specific ligand or receptor to be considered for statistical testing) to evaluate ligand and receptor (L-R) interactions amongst all annotated cell types. First, we performed this on all groups, and subsequently performed the same analysis with a “truncated mean” of 0.05 to evaluate lowly expressed immunologically relevant interactions in 5% of cells within each annotated cell type, as well as with a “truncated

mean" of 0.75 to assess major communication networks in 75% of cells. Comparative CellChat analyses were also employed to address any changes in each cell type across groups, in which the sum of probability scores for cell types of interest were also quantified in excel to highlight the incoming and outgoing interaction strength in experimental groups. Chord diagrams of signaling directionality were filtered to only include L-R signaling interactions that were at or below a p-value of 0.01. Analysis of differential number of interactions was performed to visualize the number of L-R interactions sent from one cell type to all others detected in one condition compared to the first, seen by red arrows indicating increased signaling events and blue arrows indicating decreased signaling events. Signaling pathway changes were analyzed similarly to compare major pathways utilized by a specific cell type in one condition compared to the first. Versions of additional dependencies for CellChat data visualization include NMF version 0.27 (https://github.com/renozao/NMF), circlize version 0.4.16 (https://github.com/jokergoo/circlize), and ComplexHeatmap version 2.20.0 (https://github.com/jokergoo/ComplexHeatmap).

References

1. Tacke, F. Targeting hepatic macrophages to treat liver diseases. *J. Hepatol.* **66**, 1300–1312 (2017).
2. Robinson, M. W., Harmon, C. & O'Farrelly, C. Liver immunology and its role in inflammation and homeostasis. *Cell. Mol. Immunol.* **13**, 267–276 (2016).
3. Nakashima, H. *et al.* Activation of mouse natural killer T cells accelerates liver regeneration after partial hepatectomy. *Gastroenterology* **131**, 1573–1583 (2006).
4. Tumanov, A. V *et al.* T cell-derived lymphotoxin regulates liver regeneration. *Gastroenterology* **136**, 694-704.e4 (2009).
5. Rao, R. *et al.* Interleukin 17-producing γδT cells promote hepatic regeneration in mice. *Gastroenterology* **147**, 473–84.e2 (2014).
6. Anders, R. A., Subudhi, S. K., Wang, J., Pfeffer, K. & Fu, Y.-X. Contribution of the lymphotoxin beta receptor to liver regeneration. *J. Immunol.* **175**, 1295–1300 (2005).
7. Kelly, A. *et al.* $CD141^+$ myeloid dendritic cells are enriched in healthy human liver. *J. Hepatol.* **60**, 135–142 (2014).
8. Yahoo, N., Dudek, M., Knolle, P. & Heikenwälder, M. Role of immune responses in the

development of NAFLD-associated liver cancer and prospects for therapeutic modulation. *J. Hepatol.* **79**, 538–551 (2023).
9. Foerster, F., Gairing, S. J., Müller, L. & Galle, P. R. NAFLD-driven HCC: Safety and efficacy of current and emerging treatment options. *J. Hepatol.* **76**, 446–457 (2022).
10. Llovet, J. M. *et al.* Nonalcoholic steatohepatitis-related hepatocellular carcinoma: pathogenesis and treatment. *Nat. Rev. Gastroenterol. Hepatol.* **20**, 487–503 (2023).
11. Koelsch, N. *et al.* The crosstalking immune cells network creates a collective function beyond the function of each cellular constituent during the progression of hepatocellular carcinoma. *Sci. Rep.* **13**, 12630 (2023).
12. Isbell, M. *et al.* Restoration of CD4(+) T Cells during NAFLD without Modulation of the Hepatic Immunological Pattern Is Not Sufficient to Prevent HCC. *Cancers (Basel).* **14**, (2022).
13. Mirshahi, F. *et al.* Distinct hepatic immunological patterns are associated with the progression or inhibition of hepatocellular carcinoma. *Cell Rep.* **38**, 110454 (2022).
14. Parker, T. M. *et al.* Cell competition in intratumoral and tumor microenvironment interactions. *EMBO J.* **40**, e107271 (2021).
15. Madan, E. *et al.* Flower isoforms promote competitive growth in cancer. *Nature* **572**, 260–264 (2019).
16. Guo, M., Zhang, H., Zheng, J. & Liu, Y. Glypican-3: A New Target for Diagnosis and Treatment of Hepatocellular Carcinoma. *J. Cancer* **11**, 2008–2021 (2020).
17. Teeli, A. S. *et al.* Disruption of Tumor Suppressors HNF4α/HNF1α Causes Tumorigenesis in Liver. *Cancers (Basel).* **13**, (2021).
18. Del Poggetto, E. *et al.* Epithelial memory of inflammation limits tissue damage while promoting pancreatic tumorigenesis. *Science* **373**, eabj0486 (2021).
19. Lee, H.-G. *et al.* Disease-associated astrocyte epigenetic memory promotes CNS pathology. *Nature* **627**, 865–872 (2024).
20. Aqbi, H. F. *et al.* Local and distant tumor dormancy during early stage breast cancer are associated with the predominance of infiltrating T effector subsets. *Breast Cancer Res.* **22**, 116 (2020).
21. Hu, H. *et al.* Defective efferocytosis by aged macrophages promotes STING signaling mediated inflammatory liver injury. *Cell death Discov.* **9**, 236 (2023).
22. Grabiec, A. M., Goenka, A., Fife, M. E., Fujimori, T. & Hussell, T. Axl and MerTK receptor tyrosine kinases maintain human macrophage efferocytic capacity in the presence of viral triggers. *Eur. J. Immunol.* **48**, 855–860 (2018).
23. Lhuillier, C. *et al.* Impact of Exogenous Galectin-9 on Human T Cells: CONTRIBUTION OF THE T CELL RECEPTOR COMPLEX TO ANTIGEN-INDEPENDENT ACTIVATION BUT NOT TO APOPTOSIS INDUCTION. *J. Biol. Chem.* **290**, 16797–16811 (2015).
24. Wu, C. *et al.* Galectin-9-CD44 interaction enhances stability and function of adaptive regulatory T cells. *Immunity* **41**, 270–282 (2014).
25. Chakraborty, A. *et al.* Galectin-9 bridges human B cells to vascular endothelium while programming regulatory pathways. *J. Autoimmun.* **117**, 102575 (2021).
26. Bustelo, X. R. Vav family exchange factors: an integrated regulatory and functional view. *Small GTPases* **5**, 9 (2014).
27. Dunn, S. E. *et al.* Peroxisome proliferator-activated receptor (PPAR)alpha expression in T

cells mediates gender differences in development of T cell-mediated autoimmunity. *J. Exp. Med.* **204**, 321–330 (2007).
28. Zhang, M. A. *et al.* Peroxisome proliferator-activated receptor (PPAR)α and -γ regulate IFNγ and IL-17A production by human T cells in a sex-specific way. *Proc. Natl. Acad. Sci. U. S. A.* **109**, 9505–9510 (2012).
29. Clemmons, D. R. Role of insulin-like growth factor iin maintaining normal glucose homeostasis. *Horm. Res.* **62 Suppl 1**, 77–82 (2004).
30. Huang, C.-T. *et al.* Insulin-like growth factors inhibit dendritic cell-mediated anti-tumor immunity through regulating ERK1/2 phosphorylation and p38 dephosphorylation. *Cancer Lett.* **359**, 117–126 (2015).
31. Tkachenko, E., Rhodes, J. M. & Simons, M. Syndecans: new kids on the signaling block. *Circ. Res.* **96**, 488–500 (2005).
32. Hams, E., Roberts, J., Bermingham, R. & Fallon, P. G. Functions for Retinoic Acid-Related Orphan Receptor Alpha (RORα) in the Activation of Macrophages During Lipopolysaccharide-Induced Septic Shock. *Front. Immunol.* **12**, 647329 (2021).
33. Oh, S. K. *et al.* RORα is crucial for attenuated inflammatory response to maintain intestinal homeostasis. *Proc. Natl. Acad. Sci. U. S. A.* **116**, 21140–21149 (2019).
34. Nejati Moharrami, N., Bjørkøy Tande, E., Ryan, L., Espevik, T. & Boyartchuk, V. RORα controls inflammatory state of human macrophages. *PLoS One* **13**, e0207374 (2018).
35. Han, S. *et al.* ROR alpha protects against LPS-induced inflammation by down-regulating SIRT1/NF-kappa B pathway. *Arch. Biochem. Biophys.* **668**, 1–8 (2019).
36. Kim, K. *et al.* RORα controls hepatic lipid homeostasis via negative regulation of PPARγ transcriptional network. *Nat. Commun.* **8**, 162 (2017).
37. Ho, T.-C., Yeh, S.-I., Chen, S.-L. & Tsao, Y.-P. Integrin αv and Vitronectin Prime Macrophage-Related Inflammation and Contribute the Development of Dry Eye Disease. *Int. J. Mol. Sci.* **22**, (2021).
38. Bae, H.-B. *et al.* Vitronectin inhibits efferocytosis through interactions with apoptotic cells as well as with macrophages. *J. Immunol.* **190**, 2273–2281 (2013).
39. Barbier, L. *et al.* Interleukin-1 Family Cytokines: Keystones in Liver Inflammatory Diseases. *Front. Immunol.* **10**, 2014 (2019).
40. Pradere, J.-P. *et al.* Hepatic macrophages but not dendritic cells contribute to liver fibrosis by promoting the survival of activated hepatic stellate cells in mice. *Hepatology* **58**, 1461–1473 (2013).
41. Cuño-Gómiz, C. *et al.* Sex-based differences in natural killer T cell-mediated protection against diet-induced steatohepatitis in Balb/c mice. *Biol. Sex Differ.* **14**, 85 (2023).
42. Zheng, S. *et al.* A comparative study on roles of natural killer T cells in two diet-induced non-alcoholic steatohepatitis-related fibrosis in mice. *Ann. Med.* **54**, 2233–2245 (2022).
43. Sutti, S. & Albano, E. Adaptive immunity: an emerging player in the progression of NAFLD. *Nat. Rev. Gastroenterol. Hepatol.* **17**, 81–92 (2020).
44. Zhu, H., Zhang, Q. & Chen, G. CXCR6 deficiency ameliorates ischemia-reperfusion injury by reducing the recruitment and cytokine production of hepatic NKT cells in a mouse model of non-alcoholic fatty liver disease. *Int. Immunopharmacol.* **72**, 224–234 (2019).
45. Li, X. *et al.* Integrated Single Cell Analysis Reveals An Atlas of Tumor Associated Macrophages in Hepatocellular Carcinoma. *Inflammation* (2024) doi:10.1007/s10753-

024-02026-1.
46. Sung, P. S. *et al.* Intrahepatic inflammatory IgA(+)PD-L1(high) monocytes in hepatocellular carcinoma development and immunotherapy. *J. Immunother. cancer* **10**, (2022).
47. Lurje, I., Hammerich, L. & Tacke, F. Dendritic Cell and T Cell Crosstalk in Liver Fibrogenesis and Hepatocarcinogenesis: Implications for Prevention and Therapy of Liver Cancer. *Int. J. Mol. Sci.* **21**, (2020).
48. Ngo, H. V. *et al.* Poorly Differentiated Hepatocellular Carcinoma Cells Avoid Apoptosis by Interacting with T Cells via CD40-CD40L Linkage. *Am. J. Pathol.* (2024) doi:10.1016/j.ajpath.2024.03.004.
49. Taher, T. E. *et al.* Signaling through CD44 is mediated by tyrosine kinases. Association with p56lck in T lymphocytes. *J. Biol. Chem.* **271**, 2863–2867 (1996).
50. Ilangumaran, S., Borisch, B. & Hoessli, D. C. Signal transduction via CD44: role of plasma membrane microdomains. *Leuk. Lymphoma* **35**, 455–469 (1999).
51. Kim, W.-H., Matsumoto, K., Bessho, K. & Nakamura, T. Growth inhibition and apoptosis in liver myofibroblasts promoted by hepatocyte growth factor leads to resolution from liver cirrhosis. *Am. J. Pathol.* **166**, 1017–1028 (2005).
52. Akiel, M. *et al.* IGFBP7 Deletion Promotes Hepatocellular Carcinoma. *Cancer Res.* **77**, 4014–4025 (2017).
53. Hu, Q. *et al.* Dietary fructose promotes liver carcinogenesis by inducing the malignant transformation of hepatic progenitor cells. *J. Funct. Foods* **82**, 104489 (2021).
54. Snyder, M. E. & Farber, D. L. Human lung tissue resident memory T cells in health and disease. *Curr. Opin. Immunol.* **59**, 101–108 (2019).
55. Manjili, M. H. & Manjili, S. H. The quantum model of T-cell activation: Revisiting immune response theories. *Scand. J. Immunol.* e13375 (2024) doi:10.1111/sji.13375.
56. Manjili, M. H. The Adaptation Model of Immunity: Signal IV Matters Most in Determining the Functional Outcomes of Immune Responses. *J. Immunol.* **210**, 521–530 (2023).
57. Manjili, M. H. The adaptation model of immunity: a new insight into etiology and treatment of multiple sclerosis. *Scand. J. Immunol.* e13255 (2023) doi:10.1111/sji.13255.
58. Koene, R. A. The role of adaptation in allograft acceptance. *Kidney Int.* **35**, 1073–1086 (1989).
59. Whiteside, T. L. *et al.* Evidence for local and systemic activation of immune cells by peritumoral injections of interleukin 2 in patients with advanced squamous cell carcinoma of the head and neck. *Cancer Res.* **53**, 5654–5662 (1993).
60. Barnes, J. L. *et al.* Early human lung immune cell development and its role in epithelial cell fate. *Sci. Immunol.* **8**, eadf9988 (2023).
61. Baker, C. A. & Iwasaki, A. Beyond antiviral: role of IFN-I in brain development. *Trends Immunol.* **45**, 322–324 (2024).
62. Van Der Byl, W. *et al.* The CD8(+) T cell tolerance checkpoint triggers a distinct differentiation state defined by protein translation defects. *Immunity* (2024) doi:10.1016/j.immuni.2024.04.026.
63. Sookoian, S. & Pirola, C. J. Resmetirom for treatment of MASH. *Cell* **187**, 2897-2897.e1 (2024).
64. Gao, B., Radaeva, S. & Park, O. Liver natural killer and natural killer T cells:

immunobiology and emerging roles in liver diseases. *J. Leukoc. Biol.* **86**, 513–528 (2009).
65. Li, T. *et al.* Akkermansia muciniphila suppressing nonalcoholic steatohepatitis associated tumorigenesis through CXCR6(+) natural killer T cells. *Front. Immunol.* **13**, 1047570 (2022).
66. Adler, M. *et al.* Intrahepatic natural killer T cell populations are increased in human hepatic steatosis. *World J. Gastroenterol.* **17**, 1725–1731 (2011).
67. Bhattacharjee, S. *et al.* Tumor restriction by type I collagen opposes tumor-promoting effects of cancer-associated fibroblasts. *J. Clin. Invest.* **131**, (2021).
68. Okina, Y. *et al.* TGF-β1-driven reduction of cytoglobin leads to oxidative DNA damage in stellate cells during non-alcoholic steatohepatitis. *J. Hepatol.* **73**, 882–895 (2020).
69. Asgharpour, A. *et al.* A diet-induced animal model of non-alcoholic fatty liver disease and hepatocellular cancer. *J. Hepatol.* **65**, 579–588 (2016).
70. Idowu, M. O. *et al.* CD44(+)/CD24(-/low) cancer stem/progenitor cells are more abundant in triple-negative invasive breast carcinoma phenotype and are associated with poor outcome. *Hum. Pathol.* **43**, 364–373 (2012).
71. Hao, Y. *et al.* Integrated analysis of multimodal single-cell data. *Cell* **184**, 3573-3587.e29 (2021).
72. Hu, C. *et al.* CellMarker 2.0: an updated database of manually curated cell markers in human/mouse and web tools based on scRNA-seq data. *Nucleic Acids Res.* **51**, D870–D876 (2023).
73. Guo, H. & Li, J. scSorter: assigning cells to known cell types according to marker genes. *Genome Biol.* **22**, 69 (2021).
74. Love, M. I., Huber, W. & Anders, S. Moderated estimation of fold change and dispersion for RNA-seq data with DESeq2. *Genome Biol.* **15**, 550–558 (2014).

Acknowledgment:

This work is supported by funding from NIH R01DK105961, Massey Comprehensive Cancer Center Muti-Investigator Award, grant number 2017-MIP-2, and the Office of the Assistant Secretary of Defense for Health Affairs through the Breast Cancer Research Program under Award No. W81XWH2210793. Opinions, interpretations, conclusions, and recommendations are those of the authors and are not necessarily endorsed by the U.S. Department of Defense. This work was also supported, in part, by CTSA award No. UL1TR002649 from the National Center for Advancing Translational Sciences, and from the VCU Cancer Mouse Models Core Shared Resource (CMMC) supported, in part, by funding from the NIH-NCI Cancer Center Support Grant P30 CA 016059.

Author contributions:

Conceptualization, M.H.M.; investigation, N.K., F.M., H.F.A., M.S., M.O.I.; writing first draft: N.K., M.H.M.; all authors edited the manuscript and approved the final submission; supervision: F.M., A.L.O., A.J.S, and M.H.M.; funding acquisition, M.H.M. and A.J.S. All authors reviewed the manuscript.

Data and code availability

All code and gene lists for sorting cells are available on GitHub (https://github.com/koelschnj/Systems-Approaches-Understanding-Liver-Cell-Networks-NAFLD-HCC-DietReversal) and is publicly available on the following link: https://www.ncbi.nlm.nih.gov/geo/query/acc.cgi?acc=GSE225381. The datasets generated and/or analyzed during the current study are available in the GEO repository, GSE225381.

Materials availability

DIAMOND mice used in this study will be provided, upon request to the lead contact, and may require fulfillment of an MTA. This study did not generate new unique reagents.

Declaration of interests

A.J.S. and F.M. hold a patent on the DIAMOND mouse model, PCT/US2016/056506. All other authors do not have any competing interest.

Figure legends

Figure 1: Carcinogenic events take place prior to HCC and remain dormant during recovery from HCC. A) Representative liver images and histological Hematoxylin and Eosin (H&E) staining. B) UMAP of hepatic non-immune cells (upper) and quantified non-immune cell proportions (lower). C) Heatmaps of gene expression in cancer cell and hepatocyte populations for marker genes such as Hnf4α, Afp, and Gpc3. D) Violin Plot showing log-transformed average transcript expression in the Gpc3-filtered fraction of hepatocyte and cancer cells for each group. E) Quantification of the average transcript expression level of Hnf4α+ cells in the cancer cell population in each group.

Figure 2: Hepatic cells induce macrophage and monocyte-dominated immune responses through integrins for liver tissue integrity and homeostasis. A) Immune cell proportions quantified and normalized to 100% in the CD group. B) CellChat analysis heatmap portraying results from 75% threshold analysis for Ligand (L) and Receptor (R) interactions in the CD group. C) CellChat analysis heatmap portraying results from 25% threshold analysis of L-R interactions in the CD group. D) Dominant signals detected in

75% threshold analysis depicting chord diagrams showing signaling directionality for GAS, IGF, and FN1 pathways. E) Subdominant signaling chord diagrams detected in the 25% threshold analysis for GAS, IGF, FN1, Galectin, Spp1, VTN, Collagen, Laminin, PROS, DHEAS, DHEA, IL-1, and Cholesterol pathways. F) Detection of hepatic T cell subsets with flow cytometry to differentiate T effector cells (Te, $CD44^{+}CD62L^{-/low}$), T central memory cells (Tcm, $CD44^{+}CD62L^{high}$), and T naive cells (Tn, $CD44^{-}CD62L^{+}$) in the $CD4^{+}$ and $CD8^{+}$ populations.

Figure 3: The number and strength of ligand-receptor interactions rather than cell type frequency determine the progression or inhibition of HCC. A) Quantified percentage of all immune and non-immune cells in each group. B) Comparative 75% threshold CellChat analysis quantifying the number of inferred interactions and overall interaction strength in each group. C) Cell-specific frequency (left panels) and comparative analysis in each group (right panels) with gates drawn over incoming and outgoing interaction strength values at 2 to evaluate major contributors to signaling networks.

Figure 4: HSCs, cancer cells and NKT cells dominate cellular interactions network with NKT cells orchestrating the hepatic immune responses during the progression of NAFLD on a WD. A) Quantification of cell-specific incoming and outgoing interaction strength in 75% CellChat analyses (left columns) for non-immune (upper panel) and immune cells (lower panel) in the CD and WD.nf groups, and proportional composition of each cell compartment (right columns). HSC, hepatic stellate cell; LSEC, liver sinusoidal endothelial cell; Fibro, fibroblasts; Hep, hepatocytes; Endo, endothelial cells; Cholangio, cholangiocytes; Myofibro, myofibroblasts; Neutro, neutrophils; Mac, macrophage; Mono, monocytes. B) CellChat heatmap analysis of 75% cell-cell interactions portraying all

detected L-R signaling pathways in the WD.nf group. C) The differential number of signaling events sent (left column) and received (right column) detected in HSCs, cancer cells and NKT cells encompassing 75% of cell-cell interactions during NAFLD (WD.nf) compared to the CD group. D) The differential incoming and outgoing interaction strength encompassing 75% of cell-cell interactions in the WD.nf group compared to the CD group for HSCs, cancer and NKT cells. E) Chord diagrams encompassing 75% of cell-cell interactions depicting pathways and L-R contributions for collagen, laminin, FN1, BMP, and HGF pathways in the WD.nf group. F) Chord diagrams encompassing 75% of cell-cell interactions portraying pathways and L-R contributions for galectin, PARs, testosterone, cholesterol, 27HC, and VEGF pathways in the WD.nf group.

Figure 5: The hepatic cellular interactions dominated by cancer cells, hepatocytes, myofibroblasts and fibroblasts associated with NKT cell- and monocyte-dominated immune responses during HCC on a WD. A) 75% CellChat analysis heatmap portraying all detected L-R interactions in the WD.t group (left panel), quantified incoming and outgoing interaction strength in non-immune and immune cell populations (middle panel), and proportions of non-immune and immune cells (right panel) in WD.t group. B) Dominant non-immune cell differential number of interactions sent (left column), and received (right column) in cancer, hepatocytes, myofibroblasts, and fibroblasts in WD.t compared to WD.nf. C) Dominant immune cell differential number of interactions sent (left column) and received (right column) in NKT cells and monocytes. D) 75% comparative analysis of differential incoming and outgoing interaction strength in cancer, NKT, hepatocyte, myofibroblast, fibroblast, and monocyte cell populations in WD.t compared to WD.nf.

Figure 6: Stromal cell-dominated hepatic interactions, associated with diminished immune cell engagement, promote HCC whereas myofibroblasts dominance along with monocyte-dominated immune responses, prevent HCC following dietary correction. A) 75% CellChat analysis heatmap (upper panel), quantified incoming and outgoing interaction strength for non-immune and immune cell population cell types (middle panel), and proportions of non-immune and immune cells (lower panel) in the RD.t group. B) 75% CellChat analysis heatmap (upper panel), quantified incoming and outgoing interaction strength in non-immune and immune cell populations (middle panel), and proportions of non-immune and immune cells (lower panel) in the RD.n group. C) 75% analysis showing the differential number of interactions sent (upper row) and received (lower row) for cancer, stromal cells, myofibroblasts, finroblasts and hepatocytes across multiple comparisons such as CDvRD.t (left column), CDvRD.n (middle column), and RD.tvRD.n (right column). D) 75% analysis displaying differential number of interactions sent (upper row) and received (lower row) by hepatic non-immune cells across multiple comparisons such as CDvRD.t (left column), CDvRD.n (middle column), and RD.tvRD.n (right column). E) 75% analysis displaying differential number of interactions sent (upper row) and received (lower row) by hepatic immune cells across multiple comparisons such as CDvRD.t (left column), CDvRD.n (middle column), and RD.tvRD.n (right column).

Figure 7: Stromal cell-dominated hepatic interactions, associated with diminished immune cell engagement, promote HCC whereas myofibroblasts dominance along with monocyte-dominated immune responses, prevent HCC following dietary correction. A) Signaling changes present in stromal, cancer, myofibroblasts, fibroblasts, and

hepatocyte populations in RD.t compared to CD (CD vs. RD.t; upper panel), RD.n compared to CD (CD vs. RD.n; middle panel), and in RD.n compared to RD.t (RD.t vs. RD.n; lower panel). B) Signaling changes present in NKT, NK, monocyte, and macrophage cell populations in RD.t compared to CD (CD vs. RD.t; upper panel), RD.n compared to CD (CD vs. RD.n; middle panel), and in RD.n compared to RD.t (RD.t vs. RD.n; lower panel). C) Chord diagrams depicting signaling directionality of pathways detected in 75% CellChat analyses for RD.t (upper row) and RD.n (lower row) groups.

Figure 8: Stromal cell-dominated hepatic interactions, associated with diminished immune cell engagement, promote HCC whereas myofibroblasts dominance along with monocyte-dominated immune responses, prevent HCC following dietary correction. A) Chord diagrams portraying signaling directionality of pathways detected in 75% CellChat analysis in the CD group. B) Chord diagrams demonstrating signaling directionality of various pathway detected in 75% CellChat analysis in the RD.n group. C) Chord diagram depicting Sema-3 signaling in 25% CellChat analysis in CD. D) Chord diagrams depicting signaling directionality of Complement and CypA pathways detected in 25% CellChat analysis for the RD.n group.

Figure 1

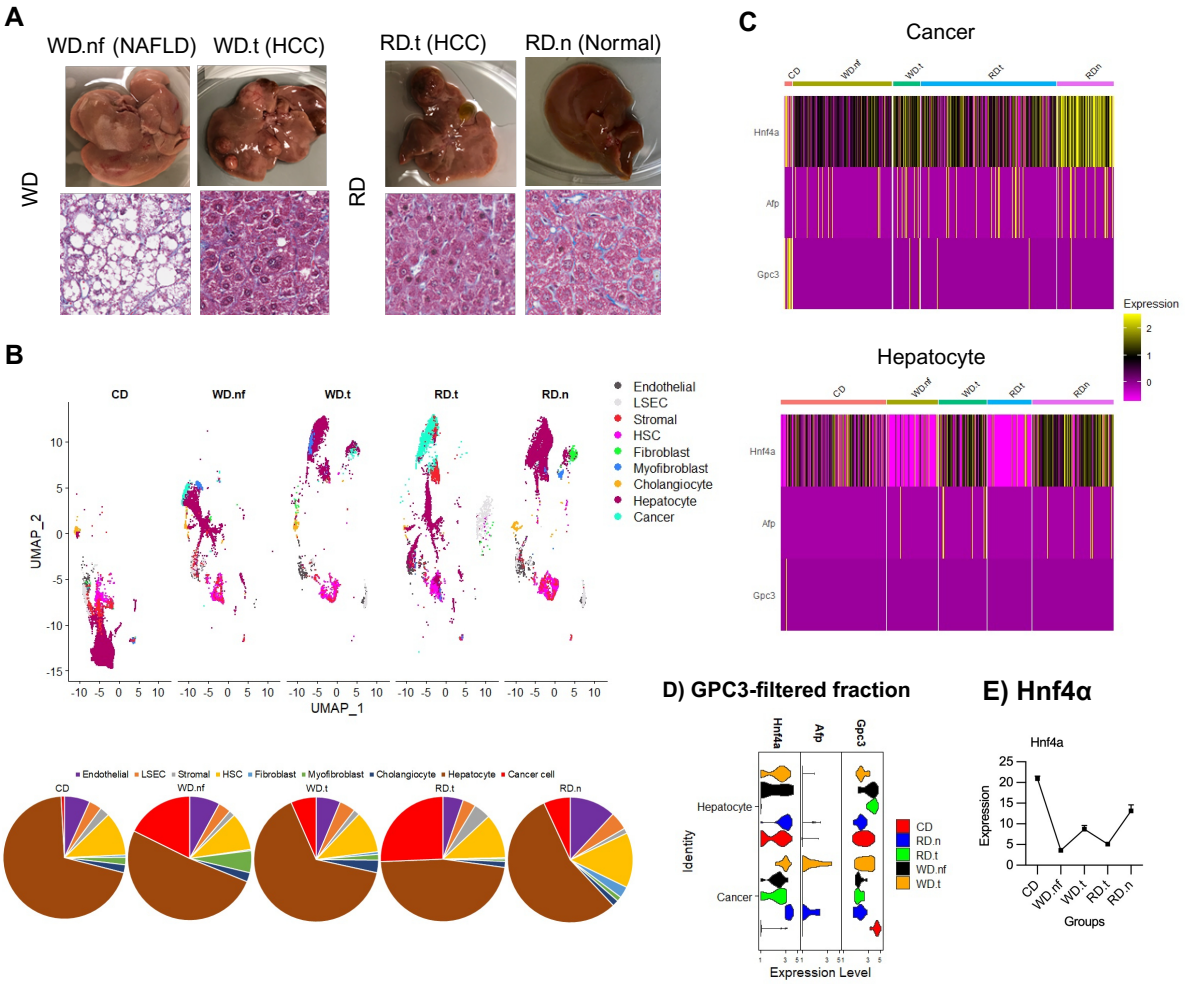
A
WD.nf (NAFLD)
WD.t (HCC)
RD.t (HCC)
RD.n (Normal)
WD
RD
B
CD
WD.nf
WD.t
RD.t
RD.n
UMAP_2
UMAP_1
Endothelial
LSEC
Stromal
HSC
Fibroblast
Myofibroblast
Cholangiocyte
Hepatocyte
Cancer
Endothelial LSEC Stromal HSC Fibroblast Myofibroblast Cholangiocyte Hepatocyte Cancer cell
C
Cancer
Hepatocyte
Hnf4a
Afp
Gpc3
Expression
D) GPC3-filtered fraction
Identity
Hepatocyte
Cancer
Expression Level
CD
RD.n
RD.t
WD.nf
WD.t
E) Hnf4α
Hnf4a
Expression
Groups

Figure 2

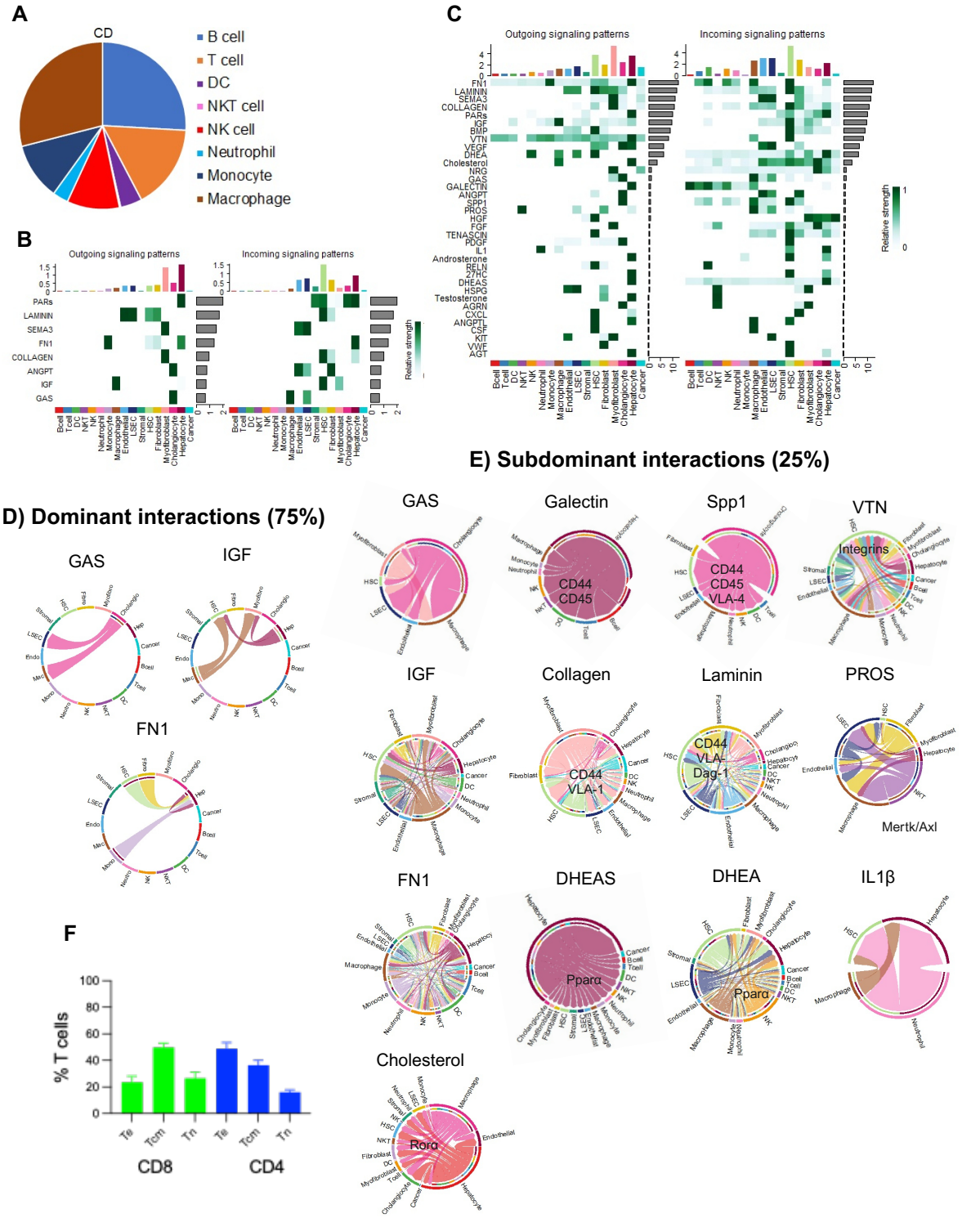
A
CD
B cell
T cell
DC
NKT cell
NK cell
Neutrophil
Monocyte
Macrophage
B
Outgoing signaling patterns
Incoming signaling patterns
PARs
LAMININ
SEMA3
FN1
COLLAGEN
ANGPT
IGF
GAS
Relative strength
C
Outgoing signaling patterns
Incoming signaling patterns
FN1
LAMININ
SEMA3
COLLAGEN
PARs
IGF
BMP
VTN
VEGF
DHEA
Cholesterol
NRG
GAS
GALECTIN
ANGPT
SPP1
PROS
HGF
FGF
TENASCIN
PDGF
IL1
Androsterone
RELN
27HC
DHEAS
HSPG
Testosterone
AGRN
CXCL
ANGPTL
CSF
KIT
VWF
AGT
Relative strength
D) Dominant interactions (75%)
GAS
IGF
FN1
E) Subdominant interactions (25%)
GAS
Galectin
CD44
CD45
Spp1
CD44
CD45
VLA-4
VTN
Integrins
IGF
Collagen
CD44
VLA-1
Laminin
CD44
VLA-
Dag-1
PROS
Mertk/Axl
FN1
DHEAS
Pparα
DHEA
Pparα
IL1β
Cholesterol
Rorα
F
% T cells
Te
Tcm
Tn
CD8
CD4

Figure 3

A) The quantified hepatic cells

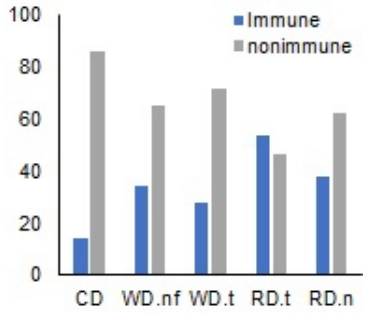

B) The quantified ligand-receptor interactions

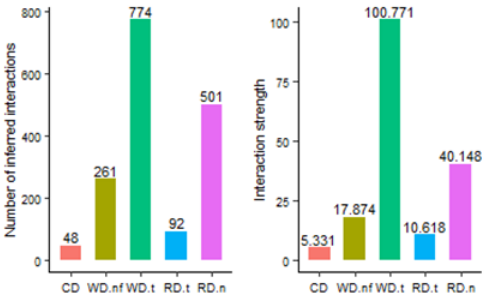

C) Cell-specific frequency & ligand-receptor interactions

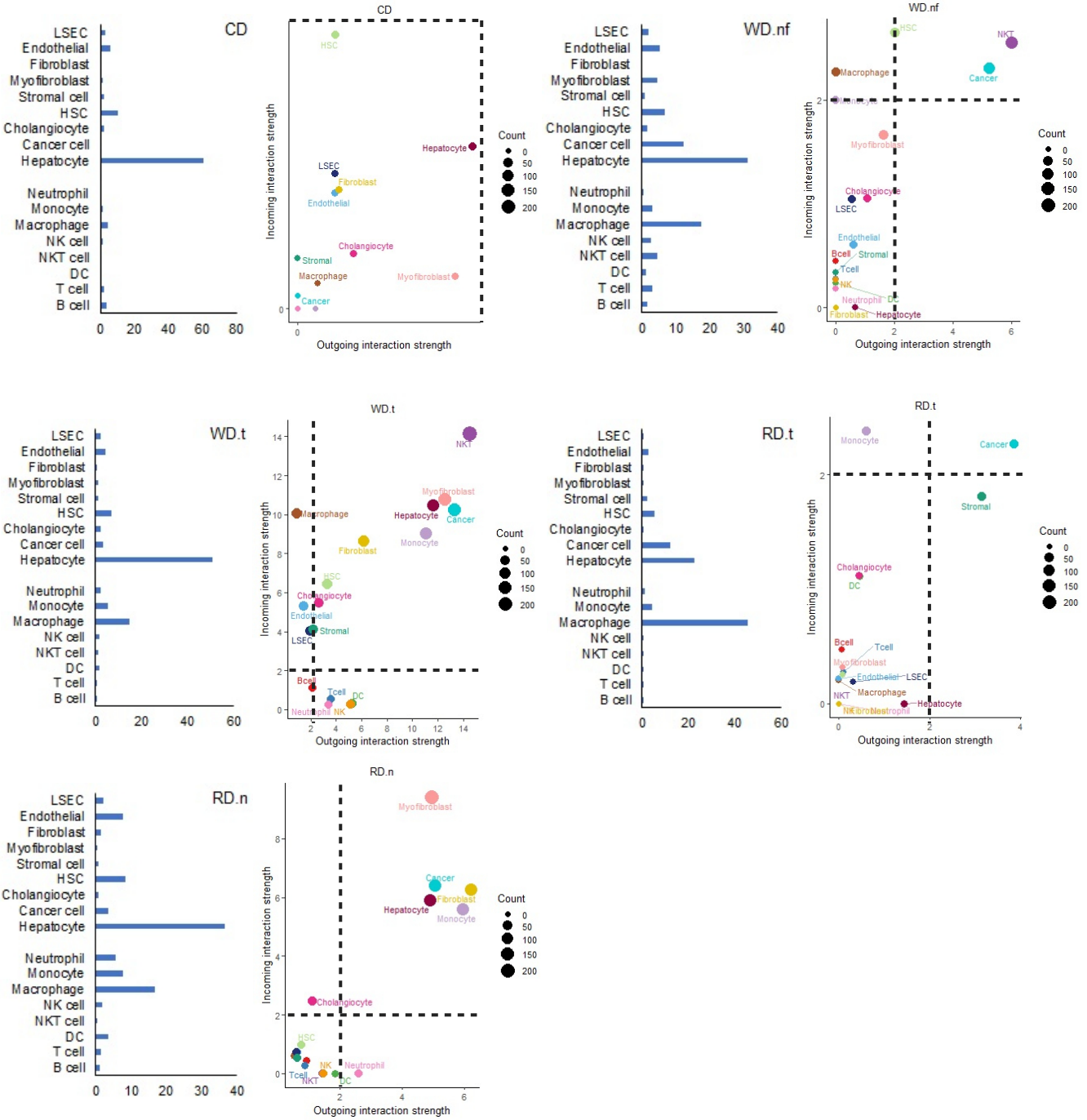

Figure 4

A) Incoming-outgoing signals

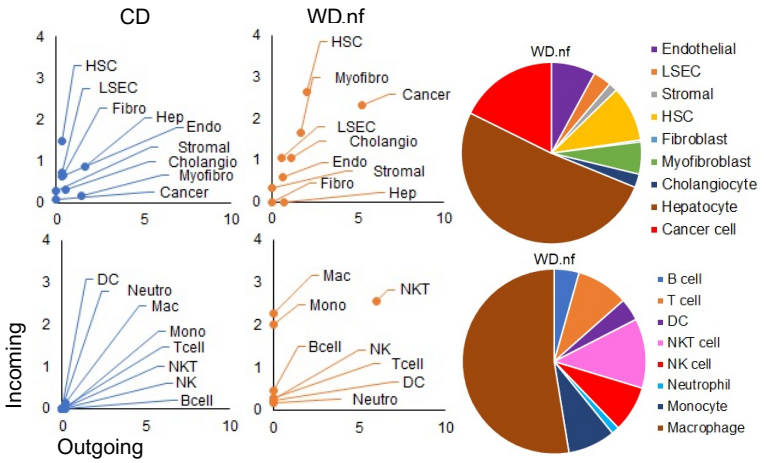

D) Hepatic homeostatic pathways

WD.nf vs. CD

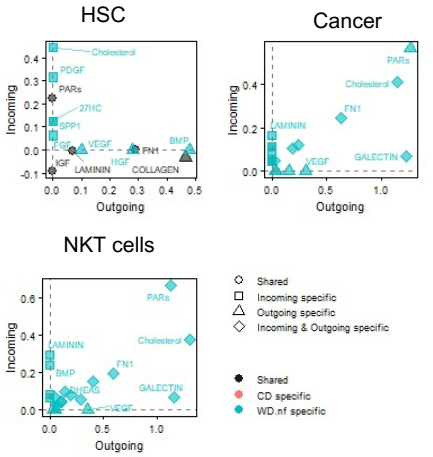

B) Ligand-receptor interactions

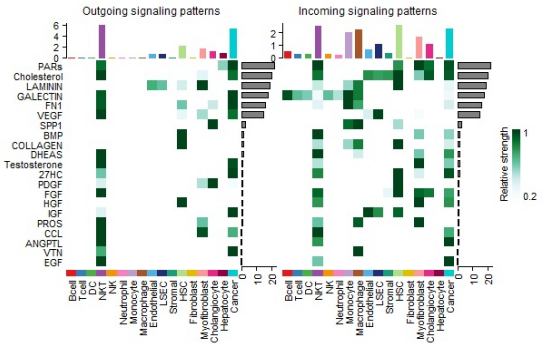

C) WD.nf vs. CD

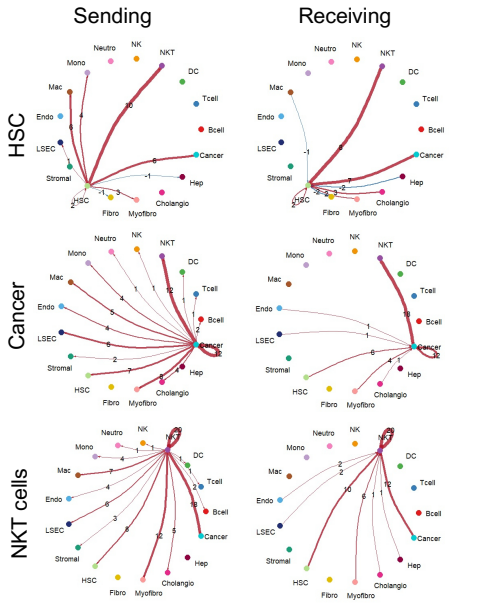

E) HSC-derived homeostatic pathways activating immune cells

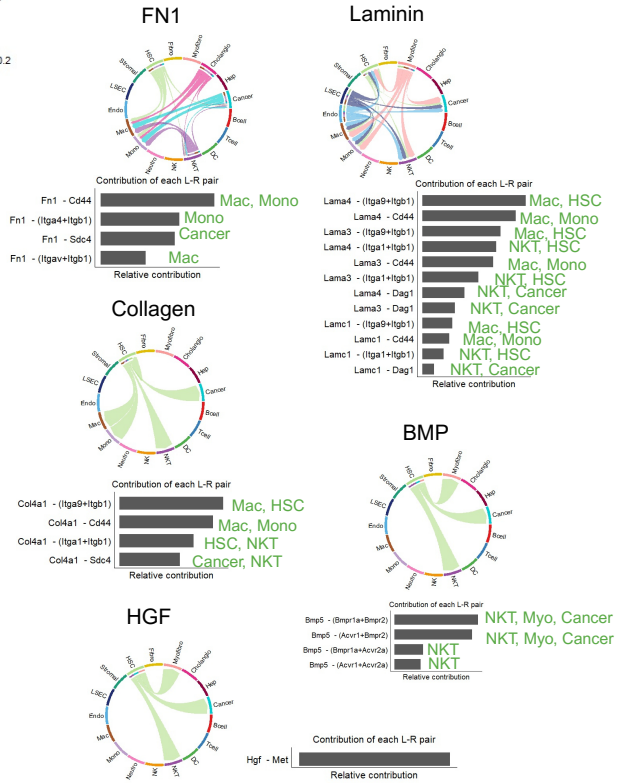

F) NKT cell and cancer cell-derived homeostatic pathways interacting with immune and non-immune cells

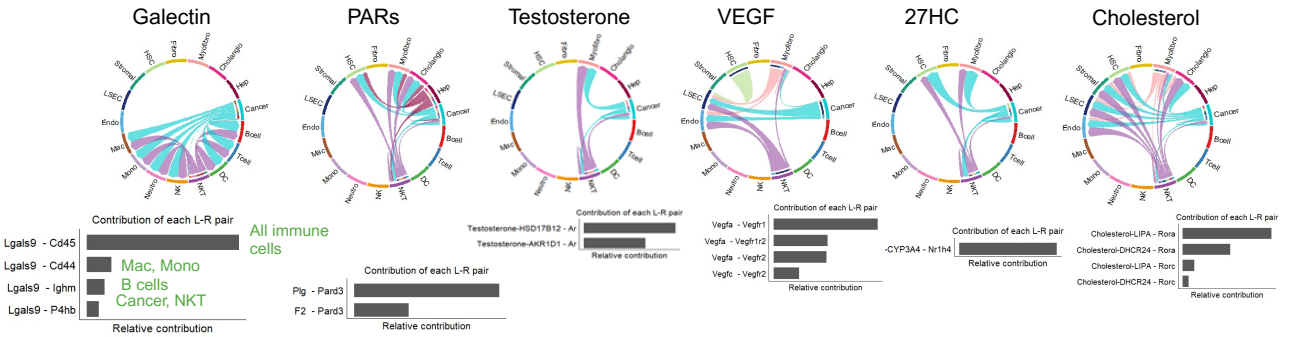

Figure 5

A) Ligand-receptor interactions network

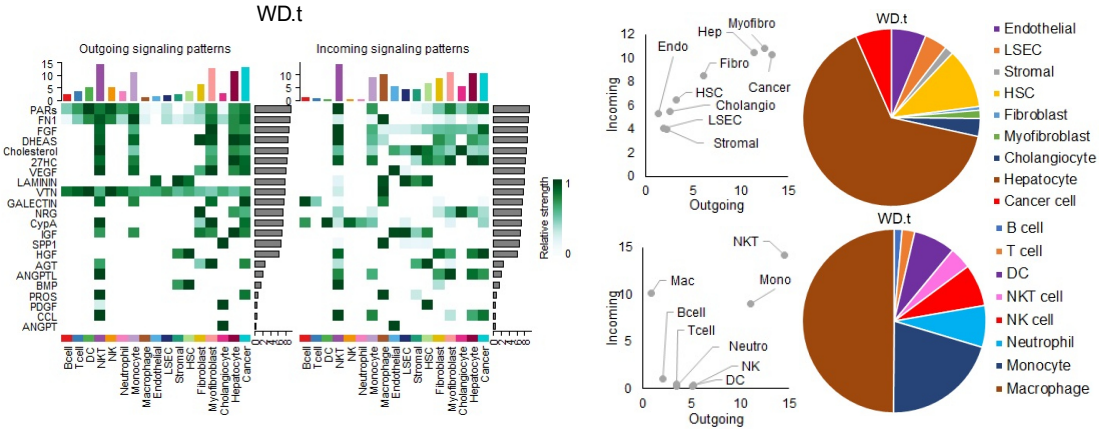

B) Nonimmune cells (WD.t vs. WD.nf)

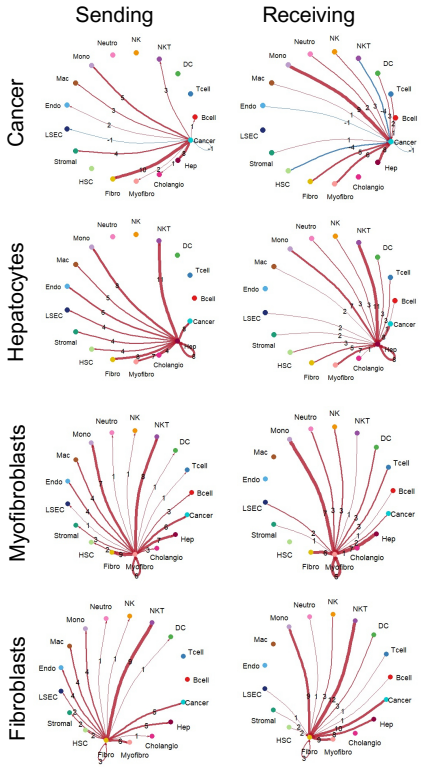

D) Signaling Pathways (WD.t vs. WD.nf)

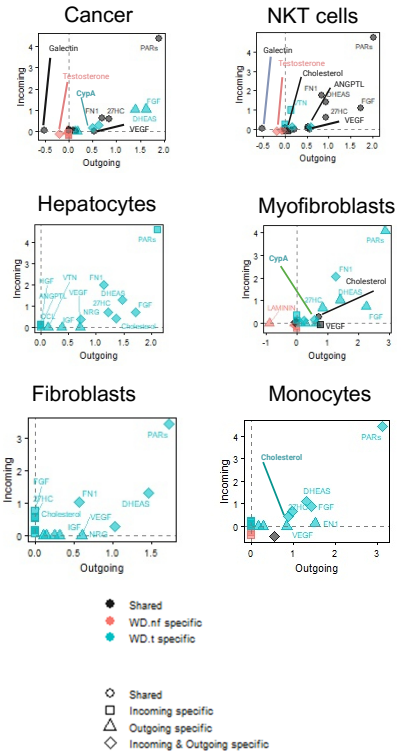

C) Immune cells (WD.t vs. WD.nf)

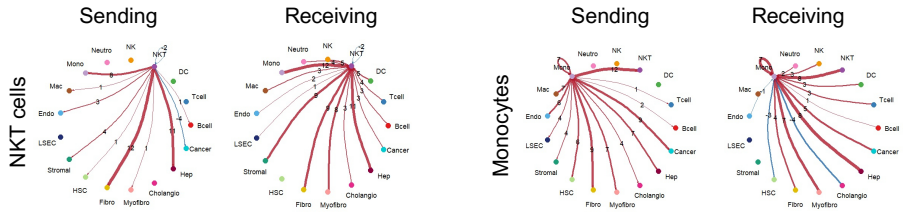

Figure 6

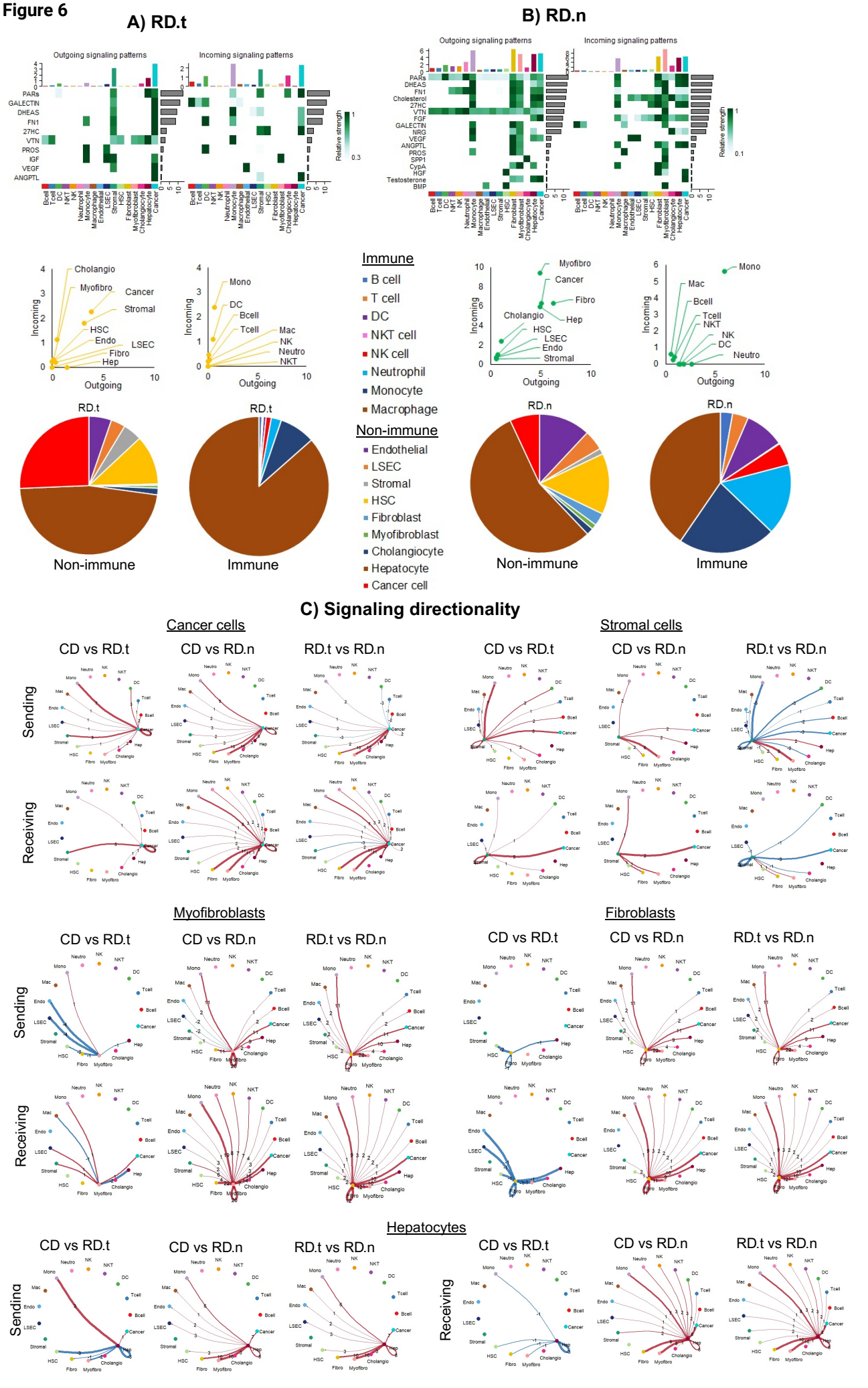
A) RD.t
B) RD.n
Outgoing signaling patterns
Incoming signaling patterns
Relative strength
Immune
B cell
T cell
DC
NKT cell
NK cell
Neutrophil
Monocyte
Macrophage
Non-immune
Endothelial
LSEC
Stromal
HSC
Fibroblast
Myofibroblast
Cholangiocyte
Hepatocyte
Cancer cell
Incoming
Outgoing
RD.t
RD.n
Non-immune
Immune
C) Signaling directionality
Cancer cells
Stromal cells
Myofibroblasts
Fibroblasts
Hepatocytes
CD vs RD.t
CD vs RD.n
RD.t vs RD.n
Sending
Receiving

Figure 6

D) Non-immune cells

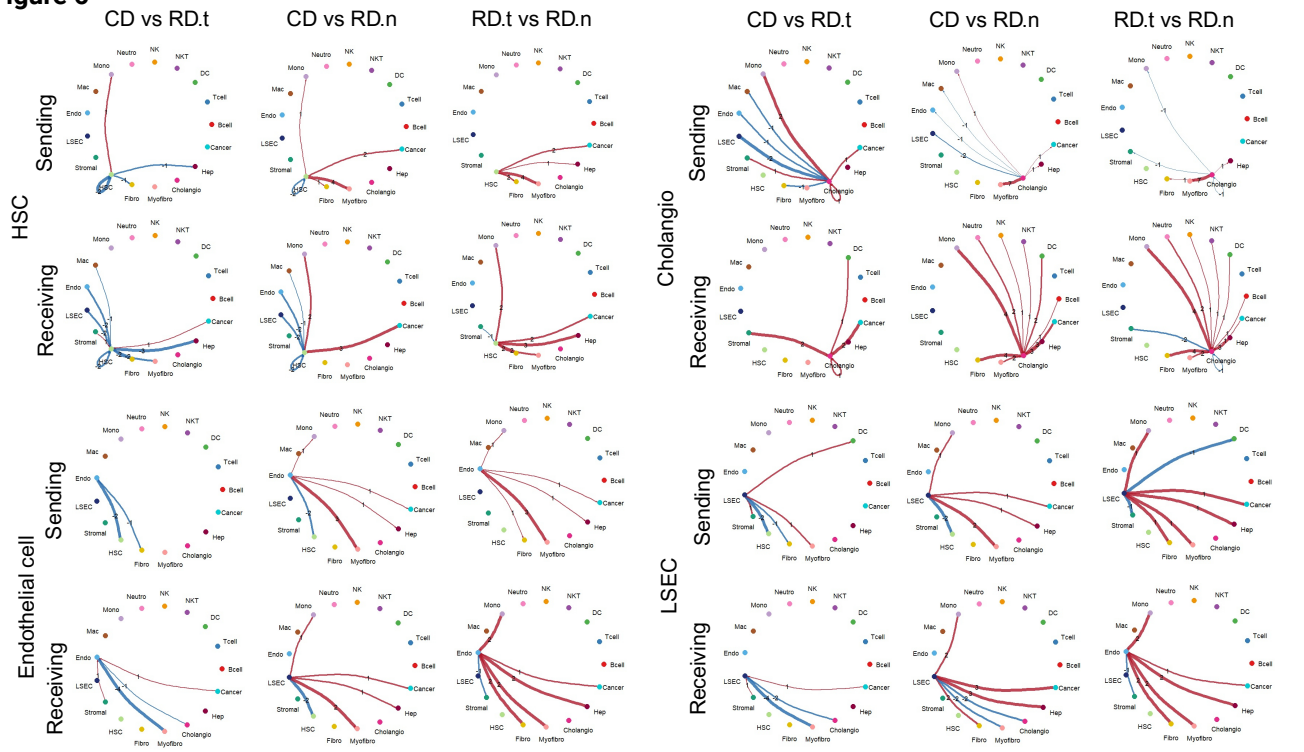

E) Immune cells

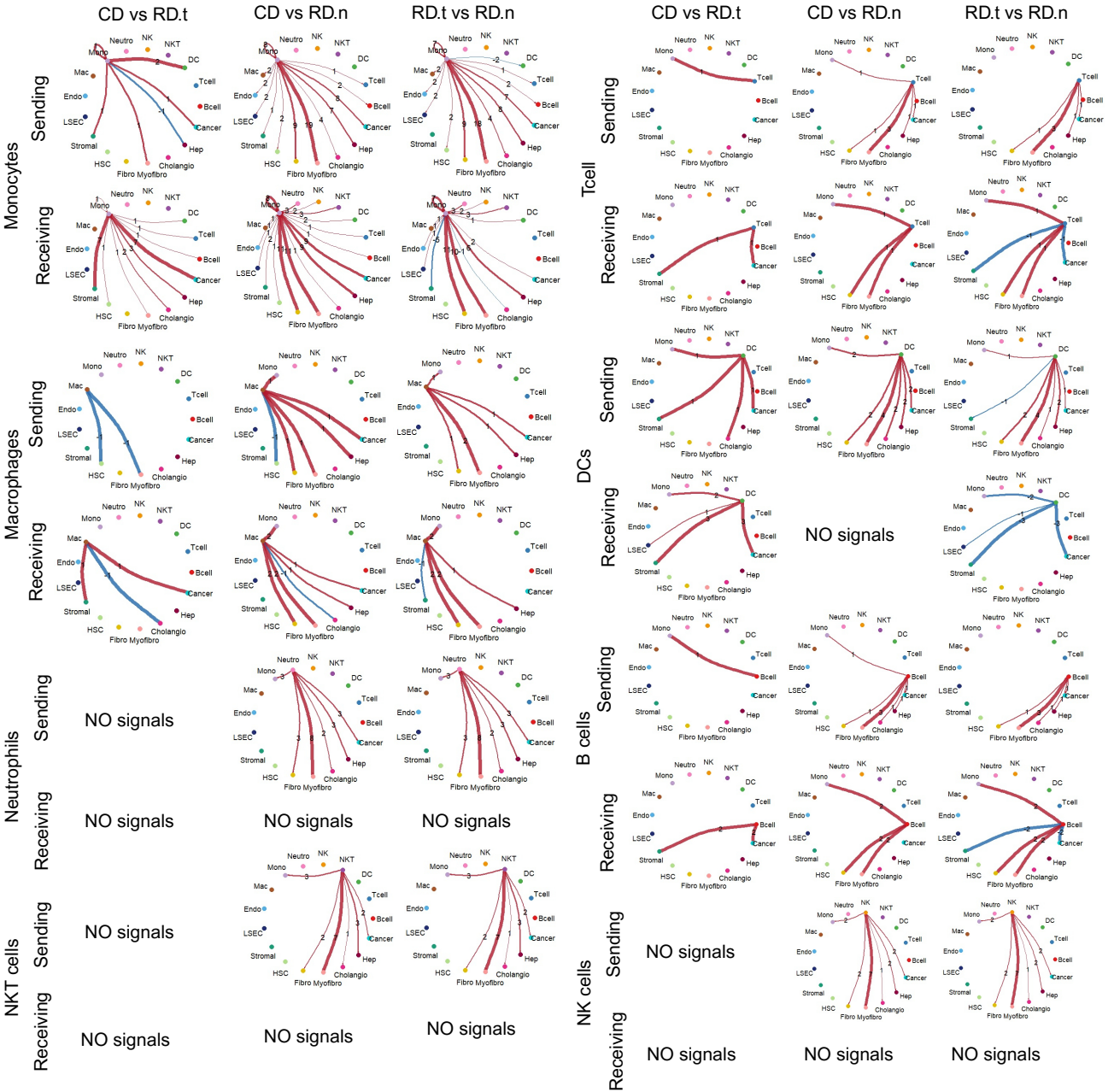

Figure 7

A) Non-immune cells

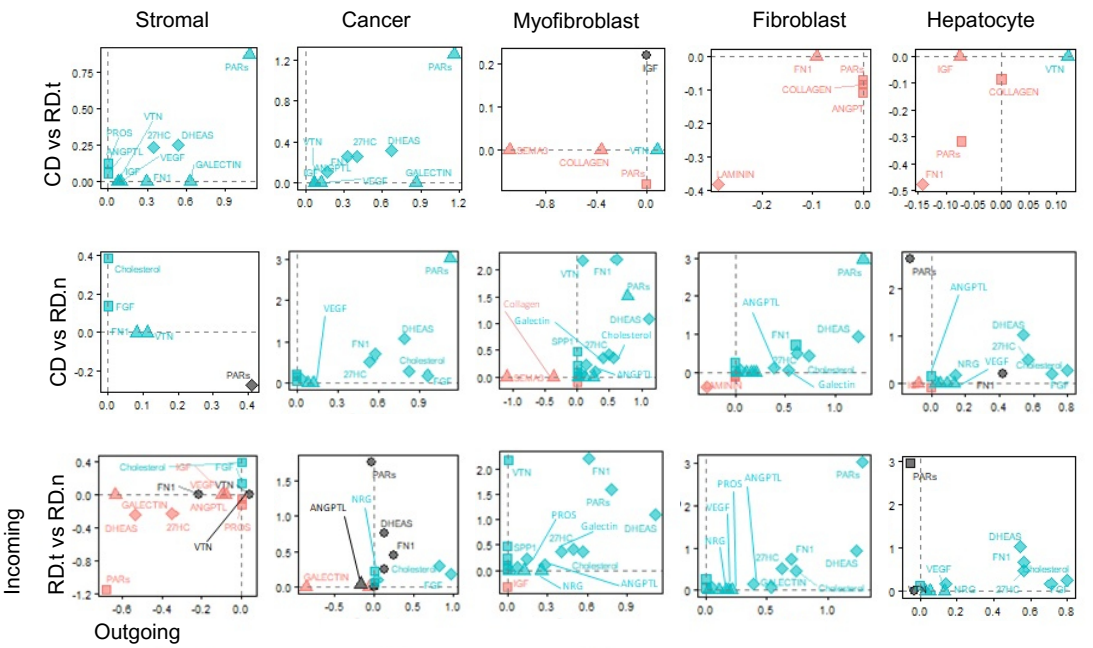

B) Immune cells

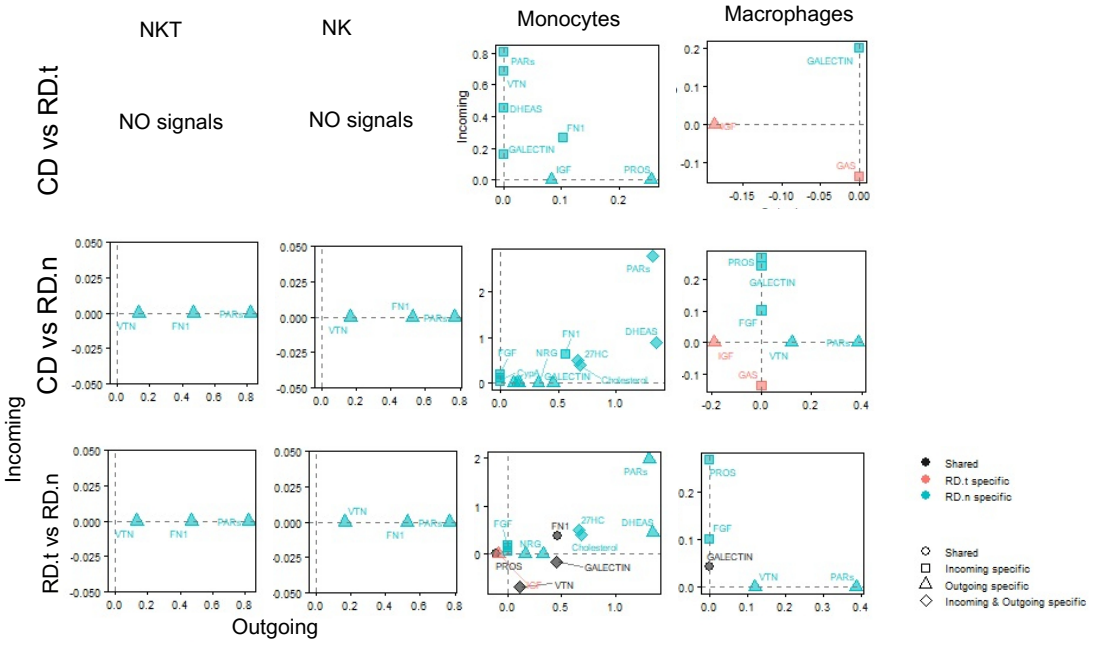

C) Signaling directionality

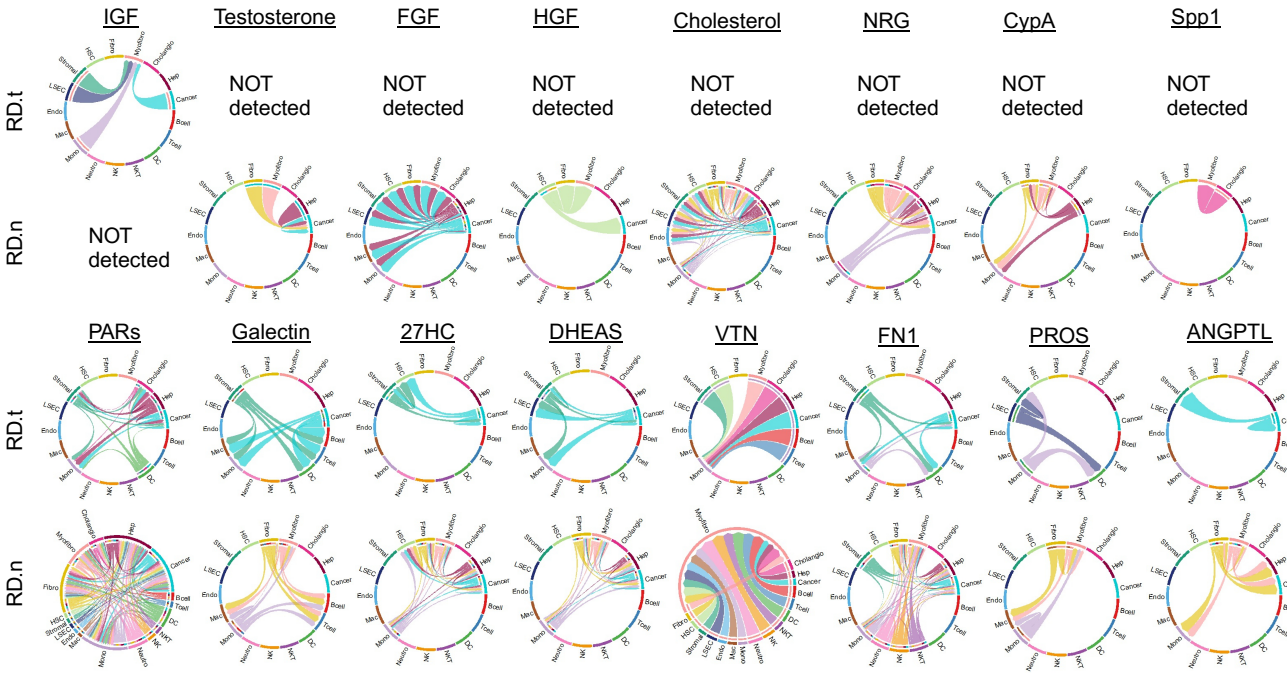

Figure 8

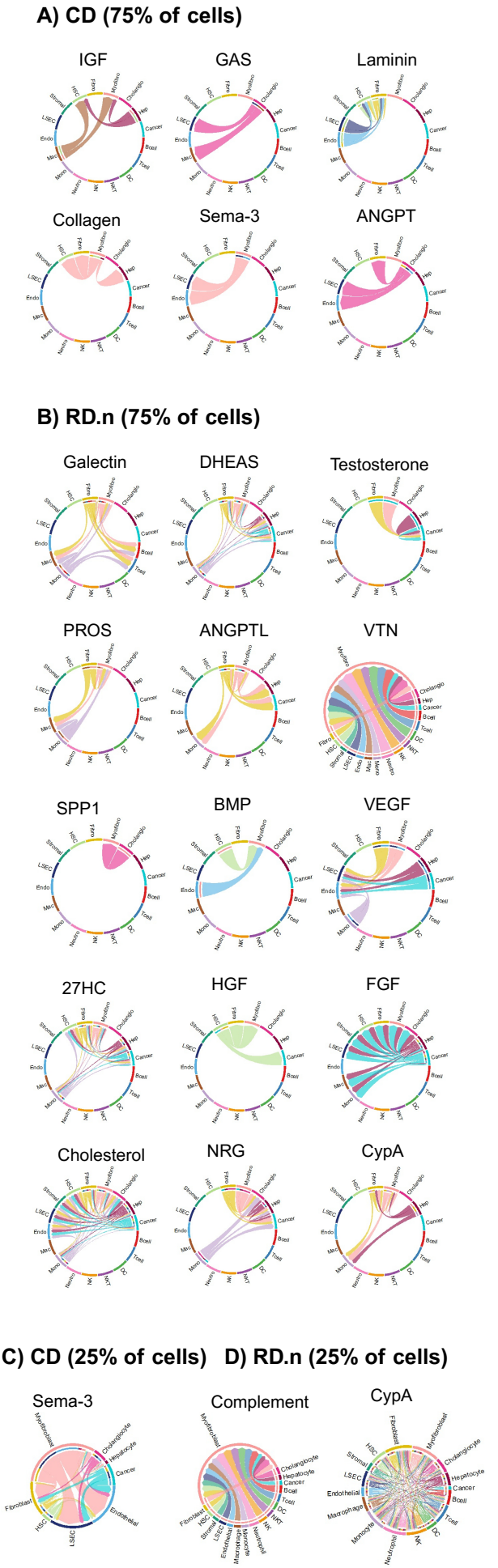
A) CD (75% of cells)
IGF
GAS
Laminin
Collagen
Sema-3
ANGPT
B) RD.n (75% of cells)
Galectin
DHEAS
Testosterone
PROS
ANGPTL
VTN
SPP1
BMP
VEGF
27HC
HGF
FGF
Cholesterol
NRG
CypA
C) CD (25% of cells)
D) RD.n (25% of cells)
Sema-3
Complement
CypA